J Neurophysiol 88: 3421–3438, 2002;
10.1152/jn.00194.2002.

Long-Term Voltage-Sensitive Dye Imaging Reveals Cortical Dynamics in Behaving Monkeys

HAMUTAL SLOVIN, AMOS ARIELI, RINA HILDESHEIM, AND AMIRAM GRINVALD
Department of Neurobiology and Grodetsky Center for Studies of Higher Brain Function, The Weizmann Institute of Science, 76100 Rehovot, Israel

Received 15 March 2002; accepted in final form 4 September 2002

Slovin, Hamutal, Amos Arieli, Rina Hildesheim, and Amiram Grinvald. Long-term voltage-sensitive dye imaging reveals cortical dynamics in behaving monkeys. *J Neurophysiol* 88: 3421–3438, 2002; 10.1152/jn.00194.2002. A novel method of chronic optical imaging based on new voltage-sensitive dyes (VSDs) was developed to facilitate the explorations of the spatial and temporal patterns underlying higher cognitive functions in the neocortex of behaving monkeys. Using this system, we were able to explore cortical dynamics, with high spatial and temporal resolution, over period of ≤1 yr from the same patch of cortex. The visual cortices of trained macaques were stained one to three times a week, and immediately after each staining session, the monkey started to perform the behavioral task, while the primary and secondary visual areas (V1 and V2) were imaged with a fast optical imaging system. Long-term repeated VSD imaging (VSDI) from the same cortical area did not disrupt the normal cortical architecture as confirmed repeatedly by optical imaging based on intrinsic signals. The spatial patterns of functional maps obtained by VSDI were essentially identical to those obtained from the same patch of cortex by imaging based on intrinsic signals. On comparing the relative amplitudes of the evoked signals and differential map obtained using these two different imaging methodologies, we found that VSDI emphasizes subthreshold activity more than imaging based on intrinsic signals, that emphasized more spiking activity. The latency of the VSD-evoked response in V1 ranged from 46 to 68 ms in the different monkeys. The amplitude of the V2 response was only 20−60% of that in V1. As expected from the anatomy, the retinotopic responses to local visual stimuli spread laterally across the cortical surface at a spreading velocity of 0.15−0.19 m/s over a larger area than that expected by the classical magnification factor, reaching its maximal anisotropic spatial extent within ~40 ms. We correlated the observed dynamics of cortical activation patterns with the monkey's saccadic eye movements and found that due to the slow offset of the cortical response relative to its onset, there was a short period of simultaneous activation of two distinct patches of cortex following a saccade to the visual stimulus. We also found that a saccade to a small stimulus was followed by direct transient activation of a cortical region in areas of V1 and V2, located retinotopically within the saccadic trajectory.

INTRODUCTION

Sensory perception and higher cortical functions emerge from intricate, dynamic interactions in very large cortical networks. Therefore to understand the function of any single cortical area or interconnected cortical areas, there is a need for a method that makes it possible to study the dynamics of the activities of neuronal populations with high spatial and temporal resolution during the performance of behavioral tasks. In principle, this need could be supplied by optical imaging based on voltage-sensitive dyes (VSDs). However, it was only after a recent series of developments in the design and synthesis of new dyes and the instrumentation for VSD imaging (VSDI) that functional imaging of cortical dynamics in anesthetized animals became feasible (Shoham et al. 1999; Tsodyks et al. 1999.) Recent intracellular recordings in vivo show that the dye signal indeed measures the sum of the membrane potential changes of all the neuronal elements in the imaged area, emphasizing changes in dendritic membrane potential simply because of the very large membrane area relative to the neuronal somata. These changes include subthreshold synaptic potentials or suprathreshold calcium and back propagating action potentials (Stuart and Sakmann 1994) in neuronal arborizations originating from neurons in all cortical layers whose dendrites reach the superficial cortical layers (Sterkin et al. 1999; see Fig. 23 in Grinvald et al. 1999).

Previous studies of the cortex of anesthetized mammals have contributed profoundly to our understanding of cortical functions at the level of single neurons and in cortical columns (Hubel and Wiesel 1962, 1969; Mountcastle 1957). However, anesthetized subjects are unsuitable for many types of studies, for example, investigation of the effects of motivation, attention, or arousal on sensory processing and perception, motor function, consciousness, and many other cognitive functions. To study the spatiotemporal cortical dynamics underlying higher cognitive functions, we developed the VSDI technique for exploration in the behaving monkey. Here we show that VSDI of the same cortical area can be used repeatedly, on a long-term basis, for a period of ≤1 yr (Slovin et al. 1999, 2000a).

Having developed this new methodological tool for use in the awake primate preparation, we explored the spatiotemporal dynamics of subthreshold/synaptic activity in neuronal populations after visual stimulation. Our objectives were the following: first, to visualize and characterize the dynamics of the functional domains (ocular-dominance columns and orientation domains) using VSDI in the visual cortex of the behaving monkey. Would the differential functional maps of these do-

Address for reprint requests: H. Slovin, Dept. of Neurobiology, The Weizmann Institute of Science, POB 26, Rehovot 76100, Israel (E-mail: hamutal.slovin@weizmann.ac.il).

The costs of publication of this article were defrayed in part by the payment of page charges. The article must therefore be hereby marked "*advertisement*" in accordance with 18 U.S.C. Section 1734 solely to indicate this fact.

mains obtained by VSDI be similar in space and amplitude to those obtained with intrinsic optical imaging (Grinvald et al. 2000; Shtoyerman et al. 2000)? Our second goal was to characterize the dynamics of the spatiotemporal VSDI responses to small local stimuli. A fundamental issue in vision is why our perception is stable even though the retinal image is rapidly changing with saccadic eye movements. Therefore the effect of saccades on multiple visual areas including primary visual area (V1) has been extensively explored (Battaglini et al. 1986; Chakraborty et al. 1998; Fischer et al. 1981; Thiele et al. 2002; Wurtz 1968 1969a,b; for review look at: Ross et al. 2001). Many researchers have reported that the threshold of visual perception is elevated during a saccade (e.g., Bridgeman et al. 1975; Latour 1962; Mackay 1970; Rigg 1974; Volkman 1962; Zuber and Stark 1966) Therefore our third goal was to start and explore the observed spatiotemporal patterns of cortical activation produced by saccadic eye movements in different regions of V1 and the secondary visual area (V2). Additional findings related saccadic eye movement in the frontal cortex, obtained with the approach described here, have been recently published (Seidemann et al. 2002). The results reported here have been published in an abstract form (Slovin et al. 1999, 2000a,b).

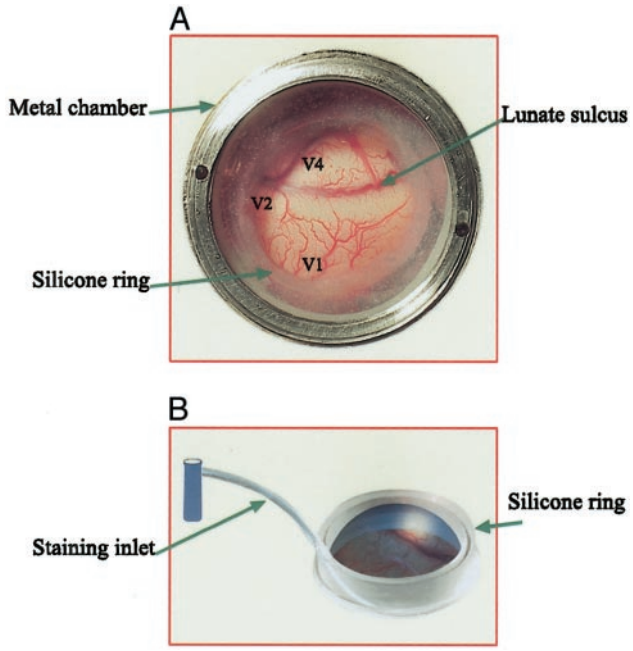

FIG. 1. Voltage-sensitive dye imaging (VSDI) cranial window and staining procedure through the artificial silicone dura. *A*: exposed cortex of *monkey Ar* seen through the special transparent silicone membrane used to stain the cortex with VSDs. The lunate sulcus is marked on the top part of the cranial window. The primary and secondary visual areas (V1 and V2) and V4 are thus available for VSDI. *B*: artificial silicone dura with an inlet tube viewed during the staining procedure. The dye is injected into the upper part of the tube, which extends further underneath the silicone ring. The tube is cut to allow the dye to emerge from it and fill the space between the cortical surface and the artificial dura. While filling this space, the dye pushes the silicone membrane upward. The tube is then sealed to prevent the dye from leaking out. The cortex is thus stained under sterile conditions over the next 2 h.

METHODS

Animals

Three adult male (6−8 kg) *Macaca fascicularis* monkeys (*M, G,* and *Ar*) were used in this study. The surgical procedure has been reported in detail previously (Arieli et al. 2002; Shtoyerman et al. 2000) and is outlined briefly in the following text.

Head holder and chambers for optical recording

All surgical procedures were performed according to the National Institutes of Health guidelines. The monkeys were anesthetized, ventilated, and provided with an intravenous catheter. A head holder and two cranial windows (25 mm ID) were placed over the primary visual cortex and cemented to the cranium with dental acrylic cement. Appropriate analgesics and antibiotics were given postoperatively.

Craniotomy, artificial dura, and routine treatment

Several months after the first procedure, the monkeys underwent a second surgical procedure in which craniotomy was performed and the dura mater was resected to expose the visual cortex. The anterior border of the exposed area was always 3−6 mm anterior to the lunate sulcus. This ensured that areas V1 and V2 were available for simultaneous imaging (Fig. 1*A*). Typically, the center of the hole was 2−4° below the representation in V1 of the horizontal meridian and 1−2° lateral to the vertical meridian. A thin, transparent silicone artificial dura with a tube (Fig. 1*B*) was implanted over the exposed cortex. The lunate sulcus was clearly visible through the transparent dura (Fig. 1*A*) as well as V1, V2, and area V4. During the entire imaging period, we opened and cleaned the chambers two to five times a week, depending on the condition of the cortex and the dura. The monkeys were awake during this painless procedure. Local and systemic antibiotics were applied according to microbiological examinations of the fluids in the chamber (Shtoyerman et al. 2000). While using antibiotics during the long period (several months) of VSDI, we did not observe any effects of the antibiotics on our results. We followed a few guidelines while using antibiotics: we used antibiotics in the chamber only when added to the agar that covered the original monkey's dura and the artificial dura and most of the antibiotics were carefully chosen to have no epileptogenic activity (e.g., quinolones). In cases that required the use of antibiotics, which could have an epileptogenic effect, (according to bacteriological sensitivity results, e.g., neomycin), we diluted the solution and mixed it only with the agar (we never washed the brain with epileptogenic antibiotics). We did not use antibiotics at any stage during recording sessions; prior to and during staining, the cortical surface was always carefully washed *only with CSF*.

Staining the cortex with new VSDs

We used a series of new oxonol VSDs, mainly RH-1691 and RH-1838. At the beginning of each VSDI session, the monkey was taken to the operating room and seated in a primate chair with its hand restrained. The chamber was open and cleaned under strict sterile conditions. The cortical surface was washed with sterile artificial cerebrospinal fluid (ACSF) and inspected to assess its condition. To ensure that the dye solution (0.2−0.3 mg/ml) was sterile, we filtered it through a 0.2 μm filter. We injected dye solution (0.5−0.6 ml) through the inlet tube of the artificial dura (Fig. 1*B*) and allowed it to drain into the chamber by carefully lifting the silicone ring of the artificial dura and enabling the dye to wash out from the cortical surface toward the chamber space. To maintain a high concentration of dye solution in contact with the cortex, we repeated this procedure three or four times, each time injecting a new dye solution and discarding the dye solution that drained from the cortical surface and was now diluted with the cortical CSF. Finally, a relatively large amount of fresh dye solution (~0.8−1.0 ml) was injected over the cortex, and this time it was not drained out. To prevent the dye from leaking to the chamber space, we sealed the silicone tube at this stage. The artificial dura together with the sealed tube provided a well-sealed

environment, and there was only a small leakage of dye solution to the chamber space (Fig. 1*B*). The rest of the chamber was then filled with the dye solution and closed. Finally, we covered the chamber to protect it from light. We were careful to avoid generating any significant pressure over the cortical surface with the dye solution because this could adversely affect normal neuronal activity.

Because CSF was circulating underneath the artificial dura, the dye solution became diluted with time. Therefore after 1 h of staining, we reopened the chamber and exchanged the dye solution over the cortex, as described in the preceding text. By maintaining the dye at the right concentration and exchanging the dye over the cortex, we were able to prevent the development of dye sediments over the cortical surface, which would severely interfere with the optical imaging. After 2 h of staining, the chamber was reopened and the cortical surface was washed with ACSF until the drained solution was as clear as the ACSF. In one monkey (*Ar*, right hemisphere), we removed the artificial dura during staining and replaced it back over the cortex at the end of the staining procedure.

To enable imaging, we now performed the following steps: hard agar solution was poured onto the real dura in the periphery of the cranial window, and a more dilute and transparent agar solution was then added on the imaging portion of the artificial dura. Overall, the procedure of staining the cortex lasted for 3–4 h (from the time that the monkey was prepared for the operation room until it was transferred to the imaging setup). Preparing the monkey in the imaging setup took another 0.5–1 h. During the entire painless staining procedure and preparation time for imaging, the monkeys were completely awake and sat calmly in their chairs. No drugs were used to sedate or calm the monkeys at any stage of the staining, preparation for imaging, or during the imaging itself.

During this period we tested eight different oxonol VSDs, three of which gave good responses: RH-1692, RH-1691, and RH-1838. RH1691/1838 appeared to give better results than the RH-1692 previously used on anesthetized cats (Shoham et al. 1999). The structures of these three blue oxonol dyes are

RH-1691

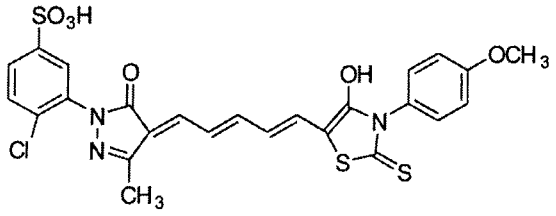

RH-1692

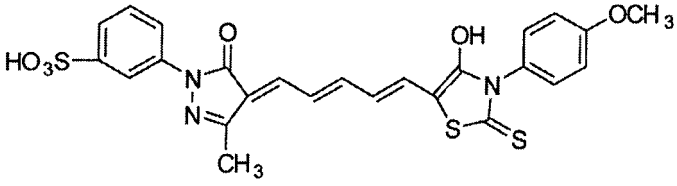

RH-1838

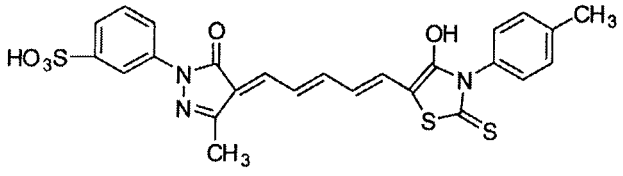

Optical imaging

The procedures of VSDI in anesthetized cats and of optical imaging of intrinsic signals in awake behaving monkeys have been discussed in detail (Shoham et al. 1999; Shtoyerman et al. 2000). Here we describe the procedure of VSDI in behaving monkeys.

Before the imaging session, the monkey was placed in a primate chair that was positioned on a carriage so that it could be rapidly transferred from the operating room to the imaging setup. The primate chair and its carriage were floating relative to the recording setup, which was stabilized by a heavy stand (~400 kg). To minimize vibration noise the following steps were taken. *1*) The monkey's head was typically fixed to the heavy stand at one point. In cases in which the monkey produced many movement artifacts during optical imaging, we fixed its head to the heavy stand using an additional point. This proved to be efficient and reduced the movement artifacts that were produced by the head movements. *2*) The monkey's hands were restrained, enabling us to obtain an electrocardiogram recording. And *3*) to further reduce any movement of the skull relative to the camera, after final focusing, the camera was connected to the monkey's head holder at two points. For real-time optical imaging we used the DyeDaq system (Shoham et al. 1999) based on the sensitive fast camera, FUJIX HR Deltron 1700, which offers a resolution of 128 × 128 pixels at 50−1,333 Hz. The exposed cortex was illuminated using an epi-illumination stage with an appropriate excitation filter (peak transmission 630 nm, width at half height 10 nm) and a dichroic mirror (DRLP 650), both from Omega Optical, Brattleboro, VT. To collect the fluorescence and reject stray excitation light, we placed a barrier postfilter above the dichroic mirror (RG 665, Schott, Mainz, Germany). Before starting the imaging, we photographed the cortex while illuminating it with a green light (540 nm bp10) to emphasize the vascular pattern. We then recorded the images, using the vascular pattern to focus the camera onto the appropriate region of the exposed cortex and to align the camera so that the imaging plane would be parallel to the cortical surface. To collect light from deeper cortical layers and reduce artifacts from the large surface vessels, we lowered the camera focus by ~400 μm. At this stage, we fixed the camera to the monkey's head, as described in the preceding text, and proceeded to collect the VSDI data for the next 3−4 h.

Behavioral paradigms

The monkeys were trained to perform two types of behavioral paradigms. The first was fixation. The trial started when the monkey fixated within 2 × 2° on a small spot of light (fixation point, 0.1 × 0.1°) that remained throughout the entire trial. After 4−6 s, a stimulus appeared on the screen. The stimulus, usually a drifting grating (contrast, 90%; size, 5−13° × 5−13°; spatial frequency, 1−3 cycles/°; temporal frequency, 1−3°/s; orientation, 0°, 90°; displayed on a computer screen, mean screen luminance 23 cd m^{-2}), was displayed for various times. The monkey had to keep fixating on the small spot until it disappeared to be rewarded with 0.2−0.3 ml of water or juice. If fixation was broken while the fixation point was lit, the trial was aborted.

To obtain real-time development of ocular-dominance functional maps, we used the following visual stimulus: a flashed square drifting grating against a black background, with spatial frequency, 1 cycle/°; temporal frequency, 3°/s; size, 13 × 13°; contrast, 90% (the background was kept black while the fixation point was lit, both when the grating was used and in the blank trials.) We also measured real-time development of the functional orientation domains of two orthogonal orientations, vertical and horizontal (VH maps), using as the visual stimulus an isoluminant square drifting grating with spatial frequency 3 cycles/°; temporal frequency, 1°/s; size, 13 × 13°; contrast, 90% (the screen background was kept isoluminant for the entire trial period, including the period of fixation prior to stimulus onset and in blank trials.) To obtain optimal functional maps, the spatial and temporal frequencies of the stimulus were set according to the frequency tuning curves of neurons in the blobs (to obtain ocular-dominance maps) or in the interblobs (to obtain VH maps) (Born et al. 1991). The control (blank) conditions that we used for this type of behavioral task were either binocular or monocular (computer-controlled shutters in front of the eyes allowed stimulation of either type).

In these trials, the monkey had to fixate as in the other trials, but no visual stimulus appeared on the screen. The monocular blank trials were used as control trials for monocularly stimulated conditions, and the binocular blank trials as control trials for binocularly stimulated conditions. We also used a blank trial version in which both eyes were covered with eye shutters. This blank condition could serve as a control trial for both monocularly and binocularly stimulated conditions but was rarely used. In the fixation paradigm, visual stimulation appeared in 67% of the trials, and 33% of the trials were control trials.

Eye position was monitored by an infrared eye tracker (Dr. Bouis Devices, Karlsruhe, Germany), sampled at 1 kHz and recorded at 200 Hz. Stimuli were presented on a 21-inch Mitsubishi monitor at 60 Hz, placed 100 cm from the monkey's eyes.

In the second behavioral task the monkey was required to make a controlled saccadic eye movement to a visual target. After achieving fixation within $2 \times 2°$ on a small spot of light ($0.1 \times 0.1°$, 4−6 s), the monkey was presented with a small drifting grating with the following properties: contrast 50%; size, $0.5-1 \times 0.5-1°$; spatial frequency, 3 cycles/°; temporal frequency, 1°/s; orientation, 0°. After a variable delay (300−2,000 ms), the fixation point disappeared, cueing the monkey to initiate a saccade toward the visual stimulus with a latency of <400−600 ms to obtain a reward. The saccade had to land within a window (not visible to the monkey) around the visual stimulus, and they tended to be accurate. Eye movements that had the typical bell-shaped velocity profile and peak velocity >100°/s were considered saccades. If fixation was broken while the fixation point was lit, the trial was aborted. The trial was also aborted if the monkey failed to make an accurate saccade within 400−600 ms of removal of the fixation point. In control trials, the monkey fixated but no stimulus was presented on the screen. As in the fixation task, 33% of the trials were control, and 67% were trials in which the visual stimulus was presented.

Behavioral control and data acquisition

Two linked personal computers were used for visual stimulation, data acquisition, and control of the monkeys' behavior. We combined our imaging software (DyeDaq) (Shoham et al. 1999) with the CORTEX software package (kindly provided by R. Desimone and E. Miller National Institutes of Health). The system was also equipped with a Sergeant Pepper Plus board (Number Nine, Lexington, MA) and a Compuboard DIO system to control the behavioral task and its data acquisition (behavior PC).

The protocol of data acquisition (DAQ) in intrinsic experiments has been described in detail elsewhere (Shtoyerman et al. 2000.) The DAQ protocol for VSDI in anesthetized animals (described in detail by Shoham et al. 1999) was modified to fit the behaving monkey protocol. Only those modifications are described here. The behavior PC controlled the fast camera through eight bits, and at the beginning of each trial, a reference image was obtained while the monkey was fixating. Data acquisition was usually begun 150−350 ms before stimulus onset and typically continued for 500−2,000 ms. The sampling rate varied between 50 and 400 frames/s. Data acquisition was triggered on the monkey's heartbeat and behavior. Stimulus onset was monitored by a photodiode and saved as an analog channel that was synchronized to DAQ. To enable analysis of single trials and to correct the jitter of the visual stimulus, each single trial was saved separately. In a typical imaging session we collected 1–2 Gb of imaging data.

Data analysis

INTRINSIC IMAGING. Functional maps were derived from the raw data by summing and dividing the frames from one or more conditions. As an example, to obtain a map of ocular dominance, we averaged the frames collected when the monkey was fixating with its left eye open and a visual stimulus was then presented and divided the resulting image by the average of the frames collected under similar conditions and during the identical time interval but with the monkey's right eye open.

VOLTAGE-SENSITIVE DYE IMAGING. For each visually stimulated condition, we calculated the evoked response, which is a series of single-condition maps (Bonhoeffer et al. 1993) corresponding to the series of acquired data frames. The recorded value at each pixel was first divided by the average value at that pixel before stimulus onset (to remove slow, stimulus-independent fluctuations in illumination and background fluorescence), and the resulting value was then divided by the value obtained for the blank condition (trials in which the monkey was fixating but no visual stimulus was presented). This procedure eliminates most of the noise due to heartbeat and respiration (Grinvald et al. 1984), and the result thus reflects evoked neuronal activity. The evoked response for monocular conditions was taken as the average of the responses to the right and left eyes. The evoked response for binocular conditions was calculated as the average of responses to all orientations. The evoked response was presented either as a time series of maps (Fig. 3*A*) or as a single time-course curve resulting from a spatial averaging over a desired cortical area, for example area V1 or V2 (Fig. 3*B*). The mapping signal for the ocular-dominance maps is defined as the difference between the two monocular evoked responses. The exact amplitude of the mapping signal was calculated in the following way: for the average ocular-dominance maps obtained by VSDI, we calculated the mean and SD of all pixels. We then chose all the pixels that had an absolute value larger than (mean +1.5 SD). In this way, we ensured that only pixels that are highly related to the functional domains were chosen, and the rest were discarded. The exact amplitude of the mapping signal for the orientation domains was calculated similarly.

Some of the maps are shown without any additional processing. In other cases, the data were weakly band-pass filtered (2D Butterworth filter; for details see figure legends). High-pass filtration was used to remove highly variable global differences in the responses to different conditions, and low-pass filtration was used to smooth the functional maps. We verified that this filtering does not alter the results.

RESPONSE LATENCY. The latency of the response to stimulus onset was calculated for time courses of single trials averaged over a specific cortical area (e.g., V1, V2). To obtain the latency of an evoked cortical response, we calculated the first derivative of the response and determined the time of its maximal amplitude $t(i)$, where i is the frame number. Then, by selecting $[t(i-1)\ldots t(i+3)]$ points, we were able to fit a linear curve on the rising phase of the evoked response curve itself (because the sampling rate was typically 9.6 ms/frame, the rising phase of the evoked response was typically only a few frames). The baseline activity was calculated as the mean value of the evoked response curve in the time points $[t(i-8)\ldots t(i-4)]$ just prior to the onset of response. Latency was defined as the first time point sampled after the intersection between the baseline and the linear curve fitted to the rising phase of the evoked response.

Minimizing photodynamic damage and pharmacological side effects

To minimize the accumulation of illumination-induced photodynamic damage, we illuminated the cortex for ≤6 s in each trial and then used a dark interstimulus interval of 8−25 s. In each VSDI session, we imaged the cortex for a total illumination time of no more than 20 min (each imaging session lasted for 3−4 h). To test for pharmacological side effects, we used intrinsic optical imaging, as described in RESULTS. To rule out pharmacological side effects of the cortical staining with the dye, we performed intrinsic optical imaging before and after the VSDI sessions. The maps of ocular-dominance columns and orientation domains were not affected by either the staining or the VSDI session. However, pharmacological side effects were observed after either prolonged staining (for >2.5 h) or staining

with a high concentration of dye solution. The side effects were manifested by a sluggish time course of response and a reduced signal-to-noise ratio. Similar phenomena were also observed in VSDI sessions that were separated by relatively short intervals (for example, in VSDI performed on a daily basis). However, these pharmacological side effects were usually reversible; after several days of recovery, during which VSDI was not performed, the dye response during the next VSDI session reverted to its normal dynamics, amplitude, and spatial patterns.

Possible contamination of the optical signals

VSDs in current use have been shown to reflect membrane-potential changes without contaminating artifacts in anesthetized cats and in cortical slices in vitro (Petersen et al. 2001). Several lines of evidence have indicated that also in the awake monkey, recording of the stimulus-evoked dye signal is not significantly contaminated by artifacts. The dye signals that we measured were restricted to the wavelength of fluorescence emission. This was tested at the end of several VSD experiments when the postfilter and dichroic mirror were removed from the macroscope and we imaged the cortex at 630 nm. Under those conditions, the fast components of the dye signal were never observed. Thus these signals are not likely to be contaminated by mechanical artifacts or rapid intrinsic signals. In addition, the rapid time course of the measured signal and the close correlation observed in other experiments between intracellular measurements and the optical signal in anesthetized cats (Sterkin et al. 1999; see Fig. 23 in Grinvald et al. 1999) rule out the possibility of significant contamination by signals from nonneuronal elements.

Duration of the recording period

Successful VSDI was sustained for a period of several months and $\leq$1 yr. This time limitation was mainly due to slow growth of a thin white tissue over the cortex, probably a proliferation of the pia mater and arachnoid mater (Arieli et al. 2002). This layer was strongly stained by the VSD, reducing penetration and staining by the dye of deep cortical layers and increasing the background fluorescence from nonneuronal elements.

RESULTS

Three hemispheres in three monkeys were successfully imaged by VSD over a period of $\leq$1 yr after removal of the dura [an average of 8.3 $\pm$ 2.0 (SE) mo]. During this period, the same cortical tissue was repeatedly stained and imaged, 1−3 times a week, $\leq$51 times from the same cortical area (an average of 32 $\pm$ 10.2 VSDI sessions per cortical area). Taken together, the three hemispheres were subjected to a total of 96 VSDI sessions. As a first step, we examined whether repeated VSDI from the same cortical area caused damage to cortical function.

Long-term repeated VSDI on the same cortical area does not modify cortical function

One of the main concerns in implementing VSDI in behaving monkeys was the possibility of causing acute and accumulated damage, either from photodynamic damage or from pharmacological side effects. To address this issue, we adopted a twofold approach. First, we tried to minimize these effects by optimizing the experimental procedures (see METHODS), and second, we assessed the condition of the cortex by evaluating its functional architecture by means of intrinsic imaging.

To evaluate the acute damage caused during a single VSDI session, at some of the recording sessions, we performed intrinsic optical imaging just before and immediately after a VSDI session. Intrinsic maps of ocular-dominance and orientation domains, obtained just before and immediately after the VSDI session, showed no differences in the spatial pattern or amplitude of the functional cortical architecture. Moreover, during a single VSDI session, the amplitude of the evoked signal was typically the same and did not decrease significantly, supporting the conclusion that normal cortical function is preserved during a VSDI session.

We also routinely performed intrinsic optical imaging ($\sim$1 to 3 times a week) during the whole period of VSDI and were thus able to compare the global time course and the functional architecture over many months while searching for evidence of accumulated damage. Even after 1 yr of VSDI we found no difference in the global time-course amplitude or functional architecture of the same cortical area; the same pattern of ocular dominance was obtained over the whole year. Figure 2 presents the functional maps of ocular-dominance (Fig. 2*A*) and orientation domains (Fig. 2*B*). Each pair of intrinsic signal maps was separated by 6 mo of VSDI. Note that the later ocular-dominance maps were obtained *after 9 mo* of VSDI (Fig. 2*A, bottom*) and the later maps of orientation domains were obtained *8 mo after* the start of VSDI (Fig. 2*B, bottom*). All of the orientation and ocular-dominance functional domains that appear in the earlier maps also appear in the later maps, and their similar shapes indicate that they did not change significantly over 6 mo [correlation coefficients (r) calculated for the 2 pairs of maps in the V1 area were 0.78 and 0.72 for the ocular-dominance and the orientation maps accordingly]. We also compared the amplitudes of the evoked response to a visual stimulus over 5 mo of VSDI and found that there was almost no change: the average response amplitude was $1.4 \times 10 \pm 0.18 \times 10$ and $1.2 \times 10 \pm 0.16 \times 10^{-3}$ (the stimulus was an isoluminant moving grating, size 0.5° located 3° below the horizontal meridian and 1.5° from the vertical meridian). In view of the preservation of the response amplitude and the similarity between the pairs of maps, particularly for the orientation maps, we concluded that the intricate cortical synaptic circuitry responsible for orientation tuning in area V1 had remained intact.

In Fig. 2*C* we show, using a different monkey, that throughout the period of VSDI the functional architecture was preserved in the entire 14-mm-diam exposed cortical area; there was no significant difference between cortical areas that were imaged with VSDI more frequently (central regions in this exposed cortical area) and less frequently (peripheral regions). There was also no significant difference in functional architecture between cortical areas that were stained more strongly and more weakly. The most noticeable difference between these two maps was the larger blood vessels artifacts masked by gray here.

Another important indication that the adverse effect of repeated VSDI is minimal was the constancy of the monkeys' behavioral performance throughout this period. If cortical function at the primary visual cortex had been significantly damaged, we would expect to find a behavioral "scotoma" specific for the location of the imaged area. However, there was no evidence of visual deficits related to the visual field represented by the imaged area while the monkeys were performing their behavioral tasks. Moreover, two of the monkeys

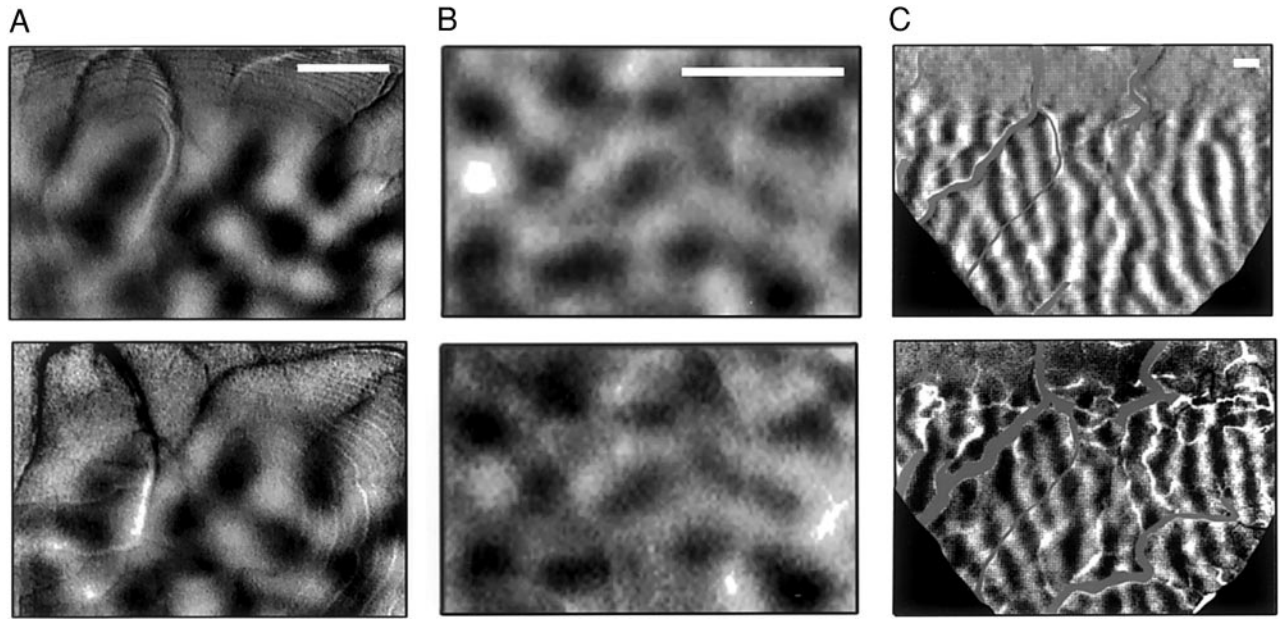

FIG. 2. Preservation of the normal cortical architecture and function throughout long-term VSDI. *A*: ocular-dominance map obtained by intrinsic imaging, 3 mo after removal of the dura and onset of VSDI (*top*) and 6 mo later (*bottom*); thus the lower map was obtained after 37 sessions of VSDI. The data are from *monkey G. B*: orientation map obtained by intrinsic imaging, 2 mo after removal of the dura and onset of VSDI (*top*) and 6 mo later (*bottom*). Thus the lower map was obtained after 29 sessions of VSDI. The cortical region from which these maps were obtained overlaps the region from which the ocular-dominance maps were obtained. The data are from *monkey G. C*: ocular-dominance map obtained by intrinsic imaging from the entire exposed cortical surface in this monkey. *Top*: obtained 1 mo after dura removal and onset of VSDI; *bottom*: obtained 3 mo later. Data are from *monkey M.* Scale bar = 1 mm.

had received further training for a more complicated controlled eye-movement task requiring the detection of subtle changes in contrast in a small (1^o) square moving grating that stimulated the imaged area retinotopically [the monkey fixated within $2 \times 2°$ on a small spot of light, $0.1 \times 0.1°$, that was turned on in the beginning of the trial. After 4−6 s, a small stimulus, size of $1 \times 1°$ drifting grating with contrast, 50%; spatial frequency, 3 cycles/°; temporal frequency, 1°/s; orientation, 0° was turned on. Following an additional variable delay (1–2 s), the monkey had to detect a subtle contrast change (from 50 to 60%) in drifting grating and respond with a saccade to the stimulus.) We compared the behavioral performance with and without dye staining and did not find a significant difference. The monkeys were able to perform the task at a high level of performance (>82%), which was not affected by the staining or by the long-term continuous VSDI. In several sessions, we also recorded the activity of single units and did not find any rough abnormal activity. Having established that VSDI does not significantly modify cortical function, we proceeded to study the spatiotemporal dynamics of visually evoked dye responses in V1 and V2.

Spatiotemporal dynamics of the evoked response in areas V1 and V2

Figure 3*A* shows a sequence of images taken after presentation of a binocular stimulus that was turned on for 1,200 ms (drifting gratings). We obtained the images by dividing each frame by a time-corresponding image from the blank condition in which the monkey was fixating but had not been given a visual stimulus so that the heartbeat pulsation artifact was eliminated. Shortly after stimulus onset there was a rapid increase in fluorescence (brightening) over the entire imaged areas of V1 and V2, corresponding to an overall depolarization of neuronal elements in the imaged areas (Fig. 3, *A* and *B*). In area V1, the response amplitude among the different VSDI sessions and monkeys varied between 0.9×10^{-3} and 2.3×10^{-3} $\Delta F/F$. In three monkeys in which the V1/V2 border was clearly observed, the amplitude of the response to a visual stimulus in V2 was typically smaller (by ~20–60%) than in V1 (Fig. 3, *A* and *B*). The latency to response onset in V1 (from stimulus onset) was highly reproducible for the same monkey over different VSDI sessions but varied among the monkeys and ranged from 46 to 68 ms (see Table 1). In many cases, the response latency in V2 was delayed by 5−15 ms compared with V1 (for example, see Fig. 3*B*). This is in agreement with previous findings (Schmolesky et al. 1998; Schroeder et al. 1998.)

Following stimulus offset, the evoked response reverted to the baseline value that had preceded visual stimulation (Fig. 3*C, top*.) To compare the rate of decrease to baseline with the rate of increase from baseline after stimulus onset, we calculated the first derivative of the averaged evoked response to a stimulus of 800-ms duration (Fig. 3*C, bottom*). In area V1, the derivative amplitude of the response to the stimulus onset was >1.5 times higher (absolute value) than that of the stimulus offset.

In one monkey, the border between areas V1 and V2 was clearly evident from the spatial activation profiles of these areas, as shown in Fig. 4, *A* and *B.* The surface plot in Fig. 4*B* shows the amplitude of the optically detected signals at each cortical site in V1 and V2 over an area of 8×8 mm^2, 150 ms after stimulus onset. At the border between the two areas, the response amplitude in V1 decreases sharply to the lower level

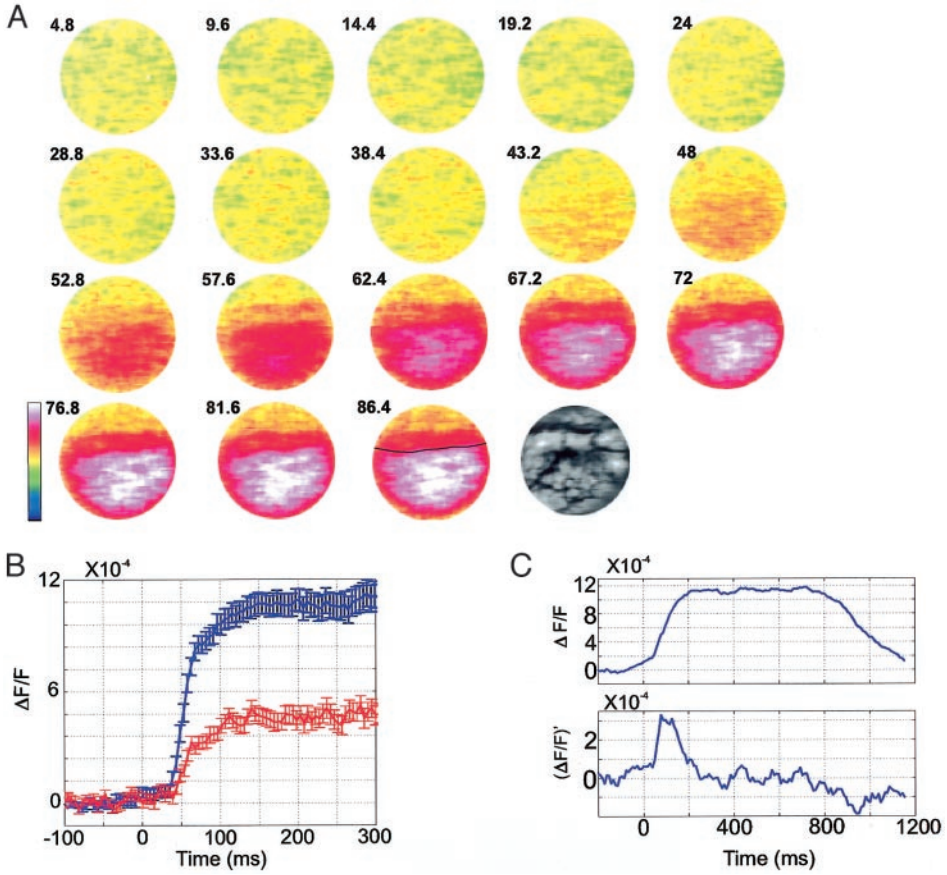

FIG. 3. Evoked response of VSD signal in area V1 and V2. *A*: a sequence of frames of the entire exposed cortical area (diameter = 14 mm), which includes both V1 and V2. The frames were obtained every 4.8 ms. Visual stimulus onset is at *time 0*. The visual stimulus was a square drifting grating with the following characteristics: size, 13 × 13°; spatial frequency, 3 cycles/°; temporal frequency, 1°/s; contrast, 90%; orientation, 90° in half of the trials and 0° in the other half. The stimulus was presented binocularly for 1,200 ms (only the images obtained during the 1st 86.4 ms are shown). The grating was isoluminant with the background. The response shown is the average of 34 trials with visual stimulation divided by the average of 22 blank trials (in which the monkey was fixating with no visual stimulus.) The dark line in the last colored frame marks the V1/V2 border, and the next black-and-white frame shows the pattern of the blood vessels from the imaged cortical area. The amplitude of the evoked response is 11×10^{-4}. *B*: the mean time course of the evoked response calculated separately for V1 (blue) and V2 (red), from the data in *A*. Time resolution is 4.8 ms. Error bars are ±SE. The onset of response in V1 was ~48 ms after stimulus onset and the response in V2 was delayed by ~10 ms. Both time courses include an initial fast response followed by a slower increase toward a plateau. Data are from *monkey M. C, top*: the evoked response in V1 to stimulus duration of 800 ms. *Bottom*: its first derivative. Absolute values of the derivative are higher for response onset than for its decay back to baseline after stimulus offset. The derivative was calculated as a sliding window size of 20 ms. The data were sampled at a resolution of 9.6 ms (n = 25 trials). Data are *from monkey G*.

seen in V2. Figure 4*A* shows that this sharp decrease corresponds to the border between V1 and V2 as revealed by a comparison with the intrinsic ocular-dominance map obtained from the same area.

Having explored the temporal aspect of the evoked response, we compared the dynamics of the evolving differential cortical maps of functional domains relative to the cortical evoked response.

Dynamics of ocular-dominance and orientation maps

To determine whether the dynamics of the ocular-dominance maps differ from the dynamics of the orientation maps, we examined the real-time development of the differential maps of both ocular-dominance and orientation domains. At present this comparison was done at a time resolution of ≤9.6 ms due to signal-to-noise ratio limitations.

TABLE 1. *Latency of evoked response in area V1*

Monkey	No. of Trials	Latency, ms
M		
Session 1	61	46.1 ± 5.2
Session 2	81	46.7 ± 6.2
Session 3	50	46.2 ± 4.9
Ar		
Session 1	16	56.6 ± 5.8
Session 2	25	57.6 ± 6.2
G		
Session 1	98	68.2 ± 6.8
Session 2	85	67.5 ± 7.5

Values are means ± SD. V1, primary visual area.

Figure 5*A* is composed of a time series of functional maps, showing the development of the ocular-dominance map itself as a function of time with a resolution of 19.2 ms/frame. To obtain the ocular-dominance maps, we used the standard approach. Figure 5*B* shows the time courses of the evoked response (blue), calculated as all monocularly stimulated conditions divided by the conditions in which both eyes were covered with eye shutters and mapping signal (red), calculated as the time course from white patches minus the time course from black patches), with a higher time resolution of 9.6 ms. The latencies of the evoked response onset and of the mapping signal are similar, ~60 ms from stimulus onset, as expected, because the ocular dominance information already exists in the thalamic input to the cortex (Hubel and Wiesel 1972). However, at late times we found a difference between the evoked response and the mapping signal: the mapping signal reached its maximal values within 40–50 ms from response onset and remained relatively constant throughout the rest of the response (Fig. 5*B*, red trace), whereas the evoked response increased throughout the response and continued to increase until ~200–280 ms after stimulus onset (Fig. 5*B*, *inset*). Therefore the fraction of the mapping signal relative to the evoked response was largest at response onset (~60%) and rapidly decreased to a low steady level of ~20% in the later part of the response. The average ocular-dominance map, shown in Fig. 5*C* (*left*), is obtained by averaging all the frames between 80 and 150 ms

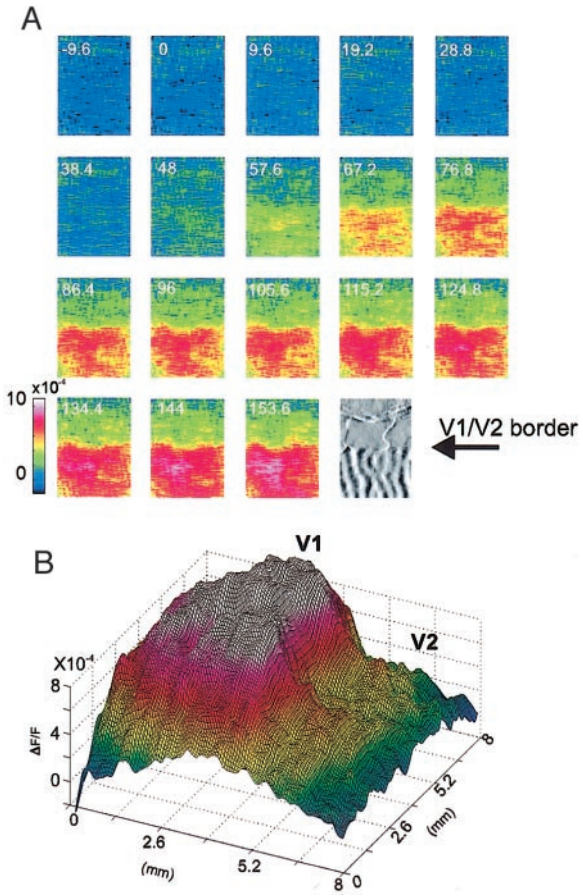

FIG. 4. Spatial profile of the evoked response in areas V1 and V2. *A*: a sequence of frames, 9.6 ms apart, obtained from V1 and V2 after stimulus onset. The amplitude of the largest response is $\sim 0.9 \times 10^{-3}$. Area V1 is activated to a higher degree than area V2. The response decreases sharply at the V1/V2 border, delineated from the intrinsic ocular-dominance map (*bottom right*); $n = 21$ and $n = 18$ for visually stimulated and blank trials, respectively. *B*: surface plot of the optically detected signals at each cortical site in V1 and V2, over an area of 8×8 mm^2, 150 ms after stimulus onset. Data are from *monkey G*.

after stimulus onset. The ocular-dominance maps obtained by VSDI had a spatial pattern similar to those obtained by imaging of the same cortical patch with intrinsic signals ($r = 0.72$, Fig. 5*C*, *right*; note that the value of r depends on signal to noise ration as well. Typically, the value of r for the same functional map, obtained in 2 subsequent imaging sessions, using the same imaging technique ranges from 0.6 to 0.9. Therefore the value of 0.7 obtained here is relatively large).

The spatial similarity of ocular-dominance maps obtained by VSDI and those obtained by intrinsic imaging reflects the large overlap in neuronal element sources that generate these differential maps. However, the fraction of the ocular-dominance maps obtained with VSDI relative to the global signal is small (only 20% at late times) compared with the relative fractional change of the ocular-dominance maps obtained with intrinsic imaging of 40–50% (Grinvald et al. 2000; Shtoyerman et al. 2000). This may suggest that intrinsic imaging is more specific to spiking activity of neuronal populations whereas VSDI reflects a larger proportion of subthreshold activity of those populations.

Next we examined the dynamics of the orientation maps (Fig. 6) to see whether they differ from the dynamics observed for the ocular-dominance map. Figure 6*A* is composed of a time series of differential maps, showing the development of the orientation map (VH map) as a function of time with a resolution of 28.8 ms/frame. To obtain the VH maps, we used the standard approach. The average VH map from the time interval of 80–300 ms following stimulus onset is shown in Fig. 6*B*. Figure 6*C* shows that the time courses of the evoked response (blue), calculated as all binocularly stimulated conditions divided by the conditions in which both eyes were covered with eye shutters and the mapping signal (red), calculated as the time course from white patches minus the time course from black patches with a higher time resolution of 9.6 ms. The latencies of the mapping signal and the evoked response were similar at this time resolution, ~60 ms. However, we found a difference in late part of the time course between the evoked response and the mapping signal. The mapping signal reached its maximal value within 40–50 ms from response onset and remained nearly constant throughout the rest of the response (Fig. 6*C*, red trace), whereas the evoked response increased throughout the response and continued to increase until ~250 ms after stimulus onset (Fig. 6*C*, *inset*). Thus the mapping signal, when expressed as a fraction of the evoked response, was largest at the beginning of the response and decreased as the evoked response continued to increase until it reached a steady level of 13% (somewhat lower than the mapping signal of the ocular-dominance map). Finally, the VH maps obtained by VSDI had a similar spatial pattern to that obtained by imaging of the same cortical area with intrinsic signals ($r = 0.7$, Fig. 6*D*).

To compare the dynamics of ocular-dominance and VH maps at low time resolution (9.6 ms/frame), we plotted the normalized mapping signal for both maps in Fig. 6*E*. Their dynamics were found to be similar. Note, however, that the relationship of the evoked signal to the mapping signal was somewhat different for orientation maps and ocular dominance maps (compare *inset* in Fig. 5*B* for ocular dominance with *inset* in Fig. 6*B* for orientation). This may be related to the different visual stimuli used to get the different maps. Our next step was to measure the cortical spatiotemporal responses to small local visual stimuli.

Retinotopic mapping of evoked responses to local stimuli in areas V1

To measure the size of the visual space that is mapped to the exposed cortical area, we presented the monkey with four different small stimuli presented in pairs (Fig. 7, *A* and *bottom right* of *B*). Figure 7*B* is composed of a time series of frames that show the development of the V1 differential retinotopic maps to two pairs of four small drifting gratings. The cortical response develops ~50 ms after stimulus onset, and the four patches that appear in V1 correspond to the four different stimuli on the screen. The differential map was calculated by dividing the frames obtained during presentation of the two vertically displaced stimuli by those obtained during presentation of the two horizontally displaced stimuli (Fig. 7*B*, a definition of the differential map is presented after the last time frame). The average map is shown in Fig. 7*C* (averaged over 70–200 ms after stimulus onset). To estimate the magnification factor for this eccentricity, we measured the distances over the cortex between the peaks of the two patches that correspond to

COLOR

FIG. 5. Dynamics of ocular-dominance maps. *A*: time series of ocular-dominance maps in V1 (differential maps are shown). Each frame is 19.2 ms long, with stimulus onset at $t = 0$. For details of stimulus, see METHODS. The response was calculated as an average of 16 trials for the ipsi eye divided by 16 trials for the contra eye. Scale bar inside the first frame is 1 mm. *B*: time course of the mapping signal (red) and of the evoked response (blue). Time resolution here was higher (than in *A*): 9.6 ms/frame. The ocular-dominance map appears as soon as the evoked response starts, ~60 ms from stimulus onset, and reaches its maximal value within 40–50 ms, after which it remains relatively constant. *Inset*: normalized evoked response and mapping signal. *C*: the average ocular-dominance map obtained by VSDI (*left*) is similar to that obtained with intrinsic signals (*right*). The data were high-and low-pass filtered. Data are from *monkey Ar*.

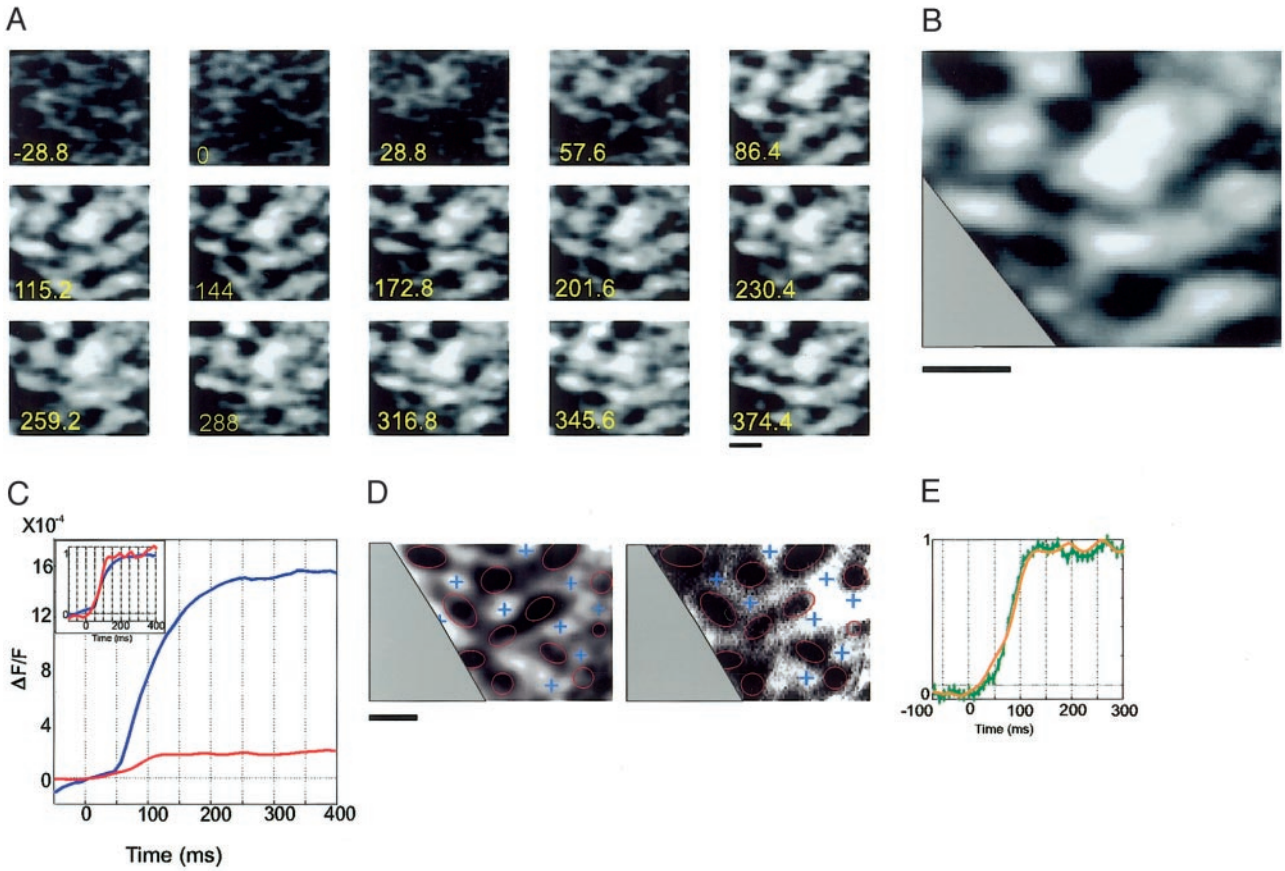

FIG. 6. Dynamics of orientation maps. *A*: real-time development of orientation domains in V1 (differential maps are shown). Each frame is 28.8 ms long. For stimulus description see text; $n = 28$ trials with horizontal orientation and $n = 27$ trials with vertical orientation. *B*: average differential orientation map obtained by VSDI. *C*: the latency of the mapping signal (red, calculated as the time course from white patches minus the time course from black patches) is similar to that of the evoked response (blue, calculated as the average of all trials with a binocular visual stimulus divided by the average of all blank trials). The time resolution here was higher (than in *A*): 9.6 ms/frame. *Inset*: normalized evoked response and mapping signal. Data are from *monkey G*. *D*: confirmation of the VSDI differential orientation map. The average orientation domain map obtained by VSDI (*left*) is similar to that obtained with intrinsic signals (*right*). The data were high-pass filtered. Data are from *monkey G*. The gray area masks blood vessel artifacts. Scale bar = 0.5 mm. *E*: normalized mapping signal of ocular-dominance (green) domains and orientation domains (orange), as a function of time (stimulus onset at $t = 0$).

the two horizontally and the two vertically displaced stimuli (1° distance between each pair of stimuli). These were found to be 3.45 and 4.43 mm, respectively. These values are close to the range of the estimated cortical magnification factor based on the results of Tootell et al. (1988) (3.0 and 4.1 mm, respectively). Thus it is possible to measure the coordinates of the exposed cortical area: the center of the chamber was roughly 2° below the horizontal meridian and 1.5° lateral to the vertical meridian.

Evoked responses to a small local stimulus in areas V1 and V2

Figure 8*A* is composed of a time series of frames showing the spatiotemporal evoked cortical response, over an area of 16 mm diam, to a small visual stimulus of 0.5 × 0.5° (location: 2° below the horizontal meridian and 1.5° from the vertical meridian) with a temporal resolution of 9.6 ms/frame. Two patches of activation appear after stimulus onset: the first patch emerges after 50 ms in V1, and one to two frames later an activation patch emerges in V2 (the border between V1 and V2 is demonstrated by the intrinsic ocular-dominance map at the *bottom right*). However, comparison of the activation between areas V1 and V2 in this case is problematic because the activation pattern in V2 becomes maximal and then abruptly declines at the lunate sulcus (Fig. 8, *A* and *B*), indicating that the V2 response is partially buried inside the lunate, and therefore we could not tell where was its peak. Figure 8*B* shows that the dye response in V1 to a small stimulus containing sharp borders does not itself have sharp borders; rather, the cortical response declines gradually as it spread laterally across the cortical surface.

Figure 9 shows a time series (temporal resolution: 9.6 ms) of vertical and horizontal spatial profiles through the center of the response (blue lines in Fig. 9*A*). The horizontal profiles are parallel to the V1/V2 border (Fig. 9*B*, *top*) and the vertical profiles are perpendicular to it (Fig. 9*B*, *bottom*). This figure shows that in area V1, within ~30–40 ms from response onset (i.e., ~80 ms after stimulus onset) the activity in response to a stimulus of 0.5° already spreads over the full extent of ~9 mm on the axis parallel to the V1/V2 border and to ~6.5 mm on the axis perpendicular to the V1/V2 border. Figure 9*C* shows the amplitude of the evoked response in area V1 and the width at

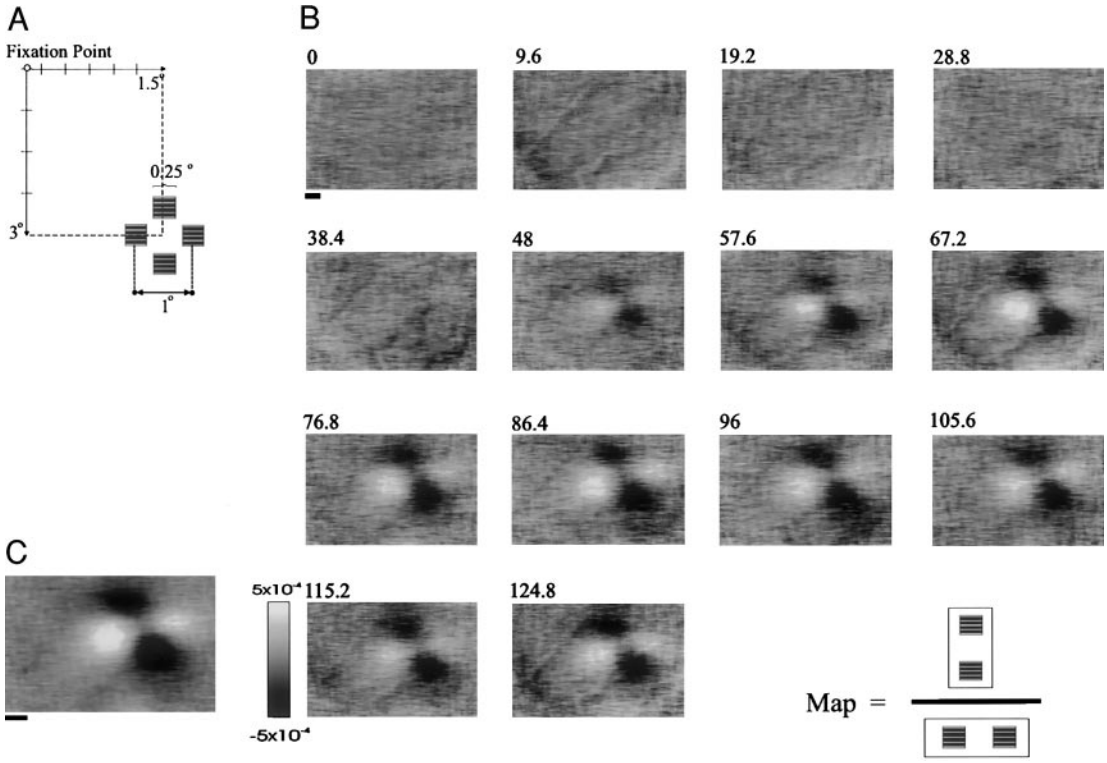

FIG. 7. VSD imaging of retinotopic activation by 4 stimuli. *A*: schematic representation of the visual stimulus. *B*: real-time development of a differential map of the response to 4 stimuli. Each frame is 9.6 ms long. The 4 patches that appear over area V1 correspond to the 4 stimuli in the matrix (see *A* for details of the stimulus). A definition of the differential map is presented after the last time frame. *C*: average differential map of a matrix of 4 stimuli ($n = 20$ trials). Data are from *monkey M*. Scale bar = 1 mm.

half-height (WHH), in V1 area alone, as a function of time for the successive spatial profiles (marked along the lines in Fig. 9*A*). The activity in V1 spreads to a WHH of 5.3 mm on the axis parallel to the vertical meridian and to 3.7 mm on the axis perpendicular to the vertical meridian. The large spread of optically detected activity appeared to cover a much larger area than that predicted by the cortical magnification factor for this eccentricity based on previous studies using classical techniques (Dow et al. 1981, Tootell et al. 1988). This large spread is characteristic of subthreshold activity, as previously shown for anesthetized monkeys using VSDI (Grinvald et al. 1994).

To compare the cortical responses for different stimulus sizes, we presented the monkey with a small moving grating square of 1 or 0.5°, located 3° below the horizontal meridian and 1.5° from the vertical meridian. In each recording session, we calculated the WHH for area V1 over an average of ~40 trials and then calculated the average over several recording sessions. Thus for a stimulus size of 1°, we calculated the WHH ($n = 4$ recording sessions) during steady state as 6.7 ± 0.2 parallel to the vertical meridian and 5.2 ± 0.2 mm perpendicular to the vertical meridian and having an amplitude of $1.2 \times 10^{-3} \pm 6 \times 10^{-5}$. For a stimulus size of 0.5°, the WHH during steady state decreased by 25–30%. Thus the WHH for a 0.5° stimulus was 5.3 ± 0.5 parallel to the vertical meridian and 3.8 ± 0.2 mm perpendicular to the vertical meridian ($n = 4$), and the amplitude was $1.1 \times 10^{-3} \pm 8 \times 10^{-5}$.

It is also evident from Fig. 9 that the evoked cortical response was anisotropic in area V1, with the longer axis located parallel to the V1/V2 border. We define the local anisotropy factor as the ratio between the spread in V1 along the axis parallel to the V1/V2 border (Fig. 9*C*, *middle*) and the spread along the axis perpendicular to the V1/V2 border (Fig. 9*C*, *bottom*). The local anisotropy factor in V1 was 1.4 for this eccentricity (Fig. 9*C*). The local anisotropic value can also be estimated from Fig. 7*B* as the ratio between the distances of the peaks on the different axes. Here we obtained an anisotropy factor of 1.3. When averaged for several recording sessions, the anisotropy factor was 1.3 ± 0.05 ($n = 8$) for a stimulus of 1° located 3° below the horizontal meridian and 1.5° from the vertical meridian. Thus the evoked optical signal was anisotropic at this eccentricity, close to the V1/V2 border, confirming previous reports using traditional techniques (Dow et al. 1985; Tootell et al. 1988; Van Essen et al. 1984).

To calculate the velocity of spread of the optically evoked signal in area V1, we calculated the average slope of WHH (parallel to the vertical meridian), over one to three frames, after response onset. The spreading velocity of the optical signal in area V1 ranged from 0.15 to 0.19 m/s, with a mean value of 0.174 ± 0.006 m/s ($n = 7$ recording sessions). These values are in agreement with previous studies (Bringuier et al. 1999; Grinvald et al.1994) and suggest that this conduction velocity is likely to be mediated by long-range nonmyelinated connections or polysynaptic pathways or feedback from higher areas. However, the spreading velocity can be defined as the first derivative in time of the WHH; in this case, the spreading velocity after a local visual stimulation contain more than one component and is dynamic with time.

Having characterized the dynamics of the responses to basic visual stimuli in areas V1 and V2, we proceeded to study the

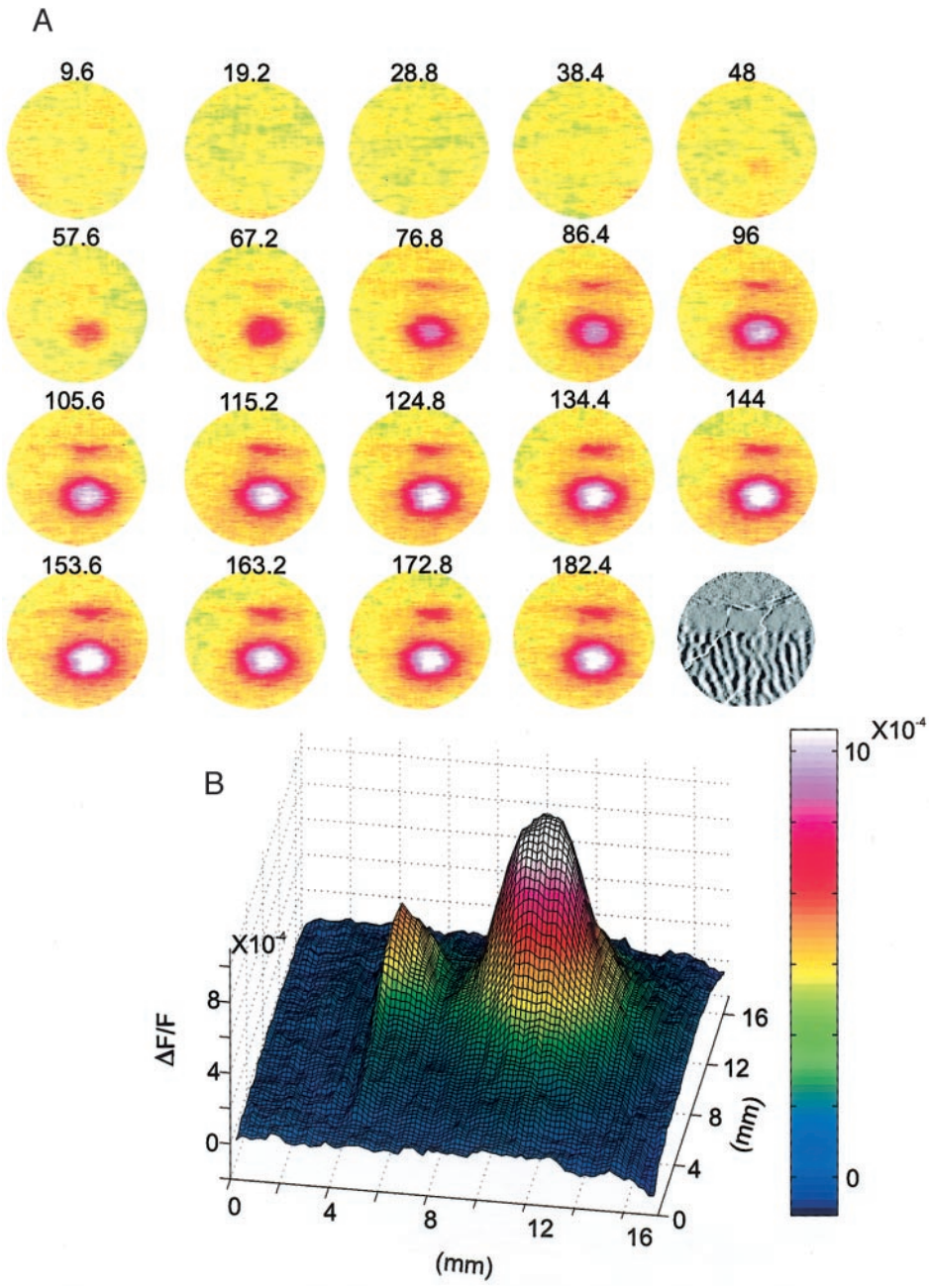

FIG. 8. Dynamics of the response to a small retinotopic visual stimulus in areas V1 and V2. *A*: spatiotemporal response to an isoluminant, small square drifting grating (size, 0.5 × 0.5°; spatial frequency, 3 cycles/°; temporal frequency, 1°/s; orientation, 0°) located 2° below the horizontal meridian and 1.5° from the vertical meridian, at a temporal resolution of 9.6 ms/frame. Stimulus onset is at $t = 0$. The maps were calculated as average of all trials ($n = 26$) in which the monkey was fixating and was presented with a visual stimulus divided by the average of all trials ($n = 23$) in which the monkey was fixating but was not presented with the visual stimulus. The border of V1/V2 was delineated from the intrinsic ocular-dominance map shown in the last panel of *A*. *B*: surface diagram plotting the amplitude of the optically detected signals at each cortical site in areas V1 and V2, over an area of 16 ×16 mm^2, for data from *A* averaged from frames obtained 80−200 ms after stimulus onset. Data are from *monkey M*.

evoked response after a simple behavior such as a saccadic eye movement.

Dynamic cortical response after a saccadic eye movement

To measure the cortical response to saccadic eye movements, we trained the monkey to perform a saccade to a small local visual stimulus (Fig. 10*A*; see METHODS for details). Figure 10*B* shows a time series of the average evoked cortical response (from 17 trials) triggered at the onset of a saccade to the small peripheral stimulus. The stimulus was turned on 500−800 ms earlier in the trial, and thus the initial frames show that before the saccade started, the retinotopic response over the cortical area was fully developed: two patches of activation appear, one in area V1 and the other in area V2. At *time 0*, the monkey made a saccade to the visual stimulus, and the visual stimulus was therefore shifted across the retina toward the fovea. Similarly, cortical activation was shifted toward a more foveal location, after a latency of ~80 ms. At this time point, however, the correlation between the temporal behavior of the stimulus and the cortical activation was disrupted: while the cortical response in the foveal location was increasing, the response in the previously responding peripheral locations (both in V1 and in V2) had not yet returned to baseline. Figure 11, *A* and *B*, shows that there is a period of ~100 ms in which two cortical regions [peripheral (cyan) and more foveal (black)] are activated simultaneously to a similar extent, i.e., for an interval of ~100 ms, the activities of the more foveal and the peripheral cortical locations overlap. During this period, the cortical activation patterns looked as if two visual stimuli were present in visual space, one at the periphery

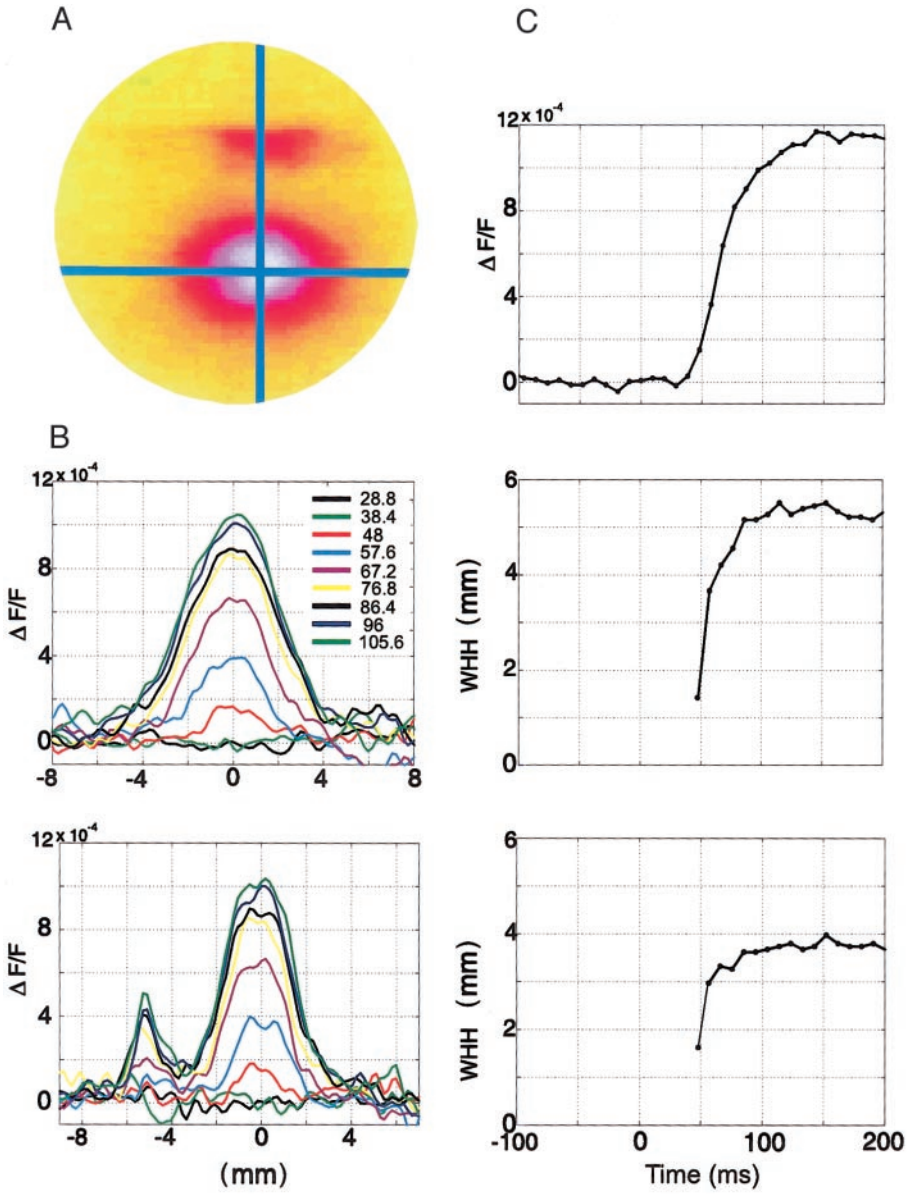

FIG. 9. Spread, magnification factor, and anisotropy in V1. *A*: location of the horizontal and vertical spatial profiles over the center of the average cortical response from Fig. 8. *B*: successive temporal displays of the spatial profiles through axes that are parallel (*top*) and perpendicular (*bottom*) to the V1/V2 border. The different colors indicate successive frames from the time of stimulus onset. The full extent of spread is ~9 mm in the axis parallel to the V1/V2 border and ~6.5 mm in the axis perpendicular to the border. *C*: evoked response as a function of time, calculated over area V1 (*top*). The figure shows the width at half-height (WHH) as a function of time for the horizontal (*middle*) and vertical spatial profiles (*bottom*), calculated only for area V1. The response spreads in an anisotropic way, and there is less spread in the axis perpendicular to the V1/V2 border than in the axis parallel to the border. Data are from *monkey M*.

and the other at the fovea, whereas on the screen there was only one visual stimulus.

We wondered whether this apparent contradiction between the cortical activation patterns and the visual stimulus, has a simple explanation. For example, the overlap of cortical activity in two completely different retinotopic locations after a saccade to a previously presented local visual stimulus may have been merely a result of the relatively slow fall-off of the cortical response to the stimulus offset (see Fig. 3*C*) that probably doesn't influence the monkey's perception. To examine this possibility, we compared the cortical fall-off response to a previously presented local visual stimulus, for two cases: after a saccade to the visual target and after the visual stimulus offset (Fig. 11*D*). We found that the cortical fall-off responses after stimulus offset and after a saccadic eye-movement do not differ significantly. Therefore the overlap of activity in two completely different cortical locations results from the slow fall-off response. We also found that another intermediate region of V1 (marked by a green square in Fig. 11*A*), which is between the two above-mentioned locations, responds to the saccadic eye movement with a transient increase in activation, which decayed rapidly (Fig. 11*B*, green curve). This region had low response amplitude prior to saccadic onset (2×10^{-4}) due to its retinotopic location relative to the stimulus position. Following a saccade, the response amplitude for this location was much smaller, and its latency appeared to be slightly shorter than the later activation at the more foveal location (black and green curves, Fig. 11, *B* and *C*), suggesting that the observed transient increase in activation does not result from spreading of activation from the most foveal region (Fig. 11*A*, black square). This finding suggests that population activity is evoked in areas V1 and V2 following a stimulus that shifts in space with saccadic velocity. However, it is not clear whether this level of activation is the same or different from what would be produced without the eye movement, an experiment that remained to be done.

Having characterized the dynamics of the response following a saccade to a visual target, we proceeded to examine the

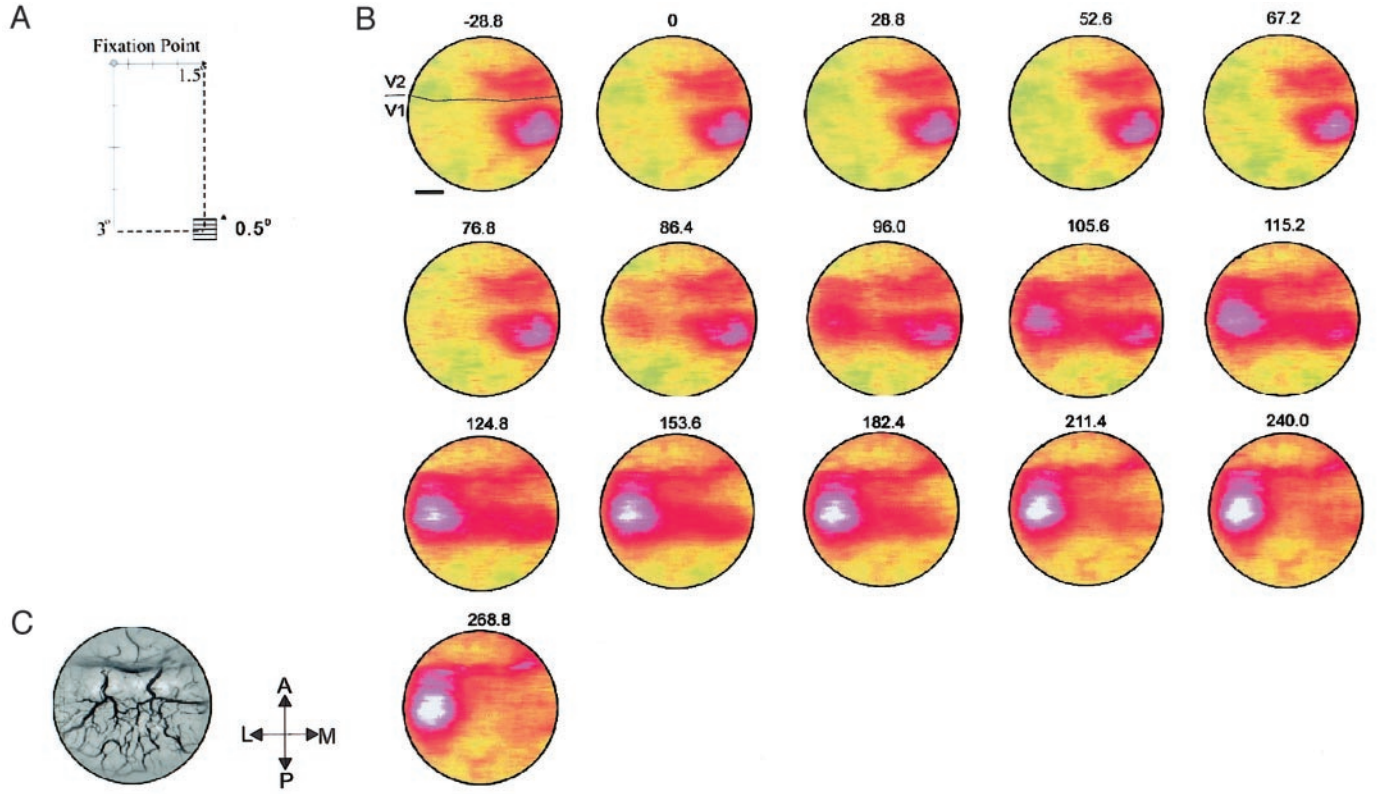

FIG. 10. Imaging of the response dynamics resulting from a saccadic eye movement. *A*: schematic representation of the visual stimulus. *B*: time series of the average optical signal triggered at the onset of a saccade to the visual stimulus ($n = 17$ trials). The first few frames show the fully developed evoked response to the small (0.5°) single isoluminant drifting grating, which was turned on 500−800 ms earlier. After a saccadic eye movement to the stimulus ($t = 0$), the activity on the cortex is shifted to a more foveal location (lateral direction). The thin black line in the first frame denotes approximately the V1/V2 border. Scale bar = 3 mm. *C*: black-and-white image of the blood vessel pattern from the imaged cortical area, measured using an ocular-dominance map obtained by intrinsic imaging. A, anterior; P, posterior; L, lateral; M, medial.

cortical response in a single trial. This was done because the detailed exploration of cortical dynamics can derive much benefit from methodologies that provide a good signal-to-noise ratio in a single trial without relying on signal averaging.

Evoked response to single trials

Single trial analysis is essential to correlate the monkey's behavior to the cortical response. Almost all of the recording sessions had a good signal-to-noise ratio in single trials, and the dye response to visual stimulation was clearly observed in these trials. Figure 12 shows typical single evoked responses to a small moving square grating in area V1, from one recording session. Blank single trials are plotted as a control for the noise level. Thus evoked responses to the visual stimulation were clearly observed on-line in response to a single presentation of the stimulus. In the present behavioral paradigm, where the monkey was simply fixating, we did not find any interesting correlation between the monkey behavior and the concomitant cortical responses in V1 and V2.

DISCUSSION

Using VSDI, we explored the spatiotemporal responses of neuronal populations to different visual stimuli. We examined the functional architecture and retinotopic dynamics of those populations as well as the cortical activity following a saccadic eye movement. The results obtained here in the behaving monkey can probably be applied, with minimal modifications, to chronic long-term VSDI in other cortical areas or many other preparations. In a recent work, we have already used long-term VSDI to investigate saccadic eye movements evoked by microstimulation in the frontal cortex of behaving monkeys (Seidemann et al. 2002). The results of the present methodological study showed that VSDI does not cause significant accumulated damage to the cortical architecture as tested by intrinsic imaging. Moreover, we demonstrated the ability to obtain single-trial results with a high signal-to-noise ratio and were able to clearly observe on-line evoked responses to the visual stimulation after a single presentation of the stimulus (Fig. 12). This latter ability would be particularly important for the study of behavior and cortical dynamics. However, the noise in the awake monkey is larger than that we observed in VSDI imaging on anesthetized animals. Thus it remains important to improve the dyes further or to develop a new analytical approach to remove the biological noise that occurs in awake animal and not in the anesthetized monkey.

Effects of long-term VSDI in behaving monkeys

The short- and long-term effects of cortical VSDI on cortical activity were examined by intrinsic functional mapping of the visual cortex over a period of many months. We showed in this study that throughout the entire period of the VSDI, the spatial

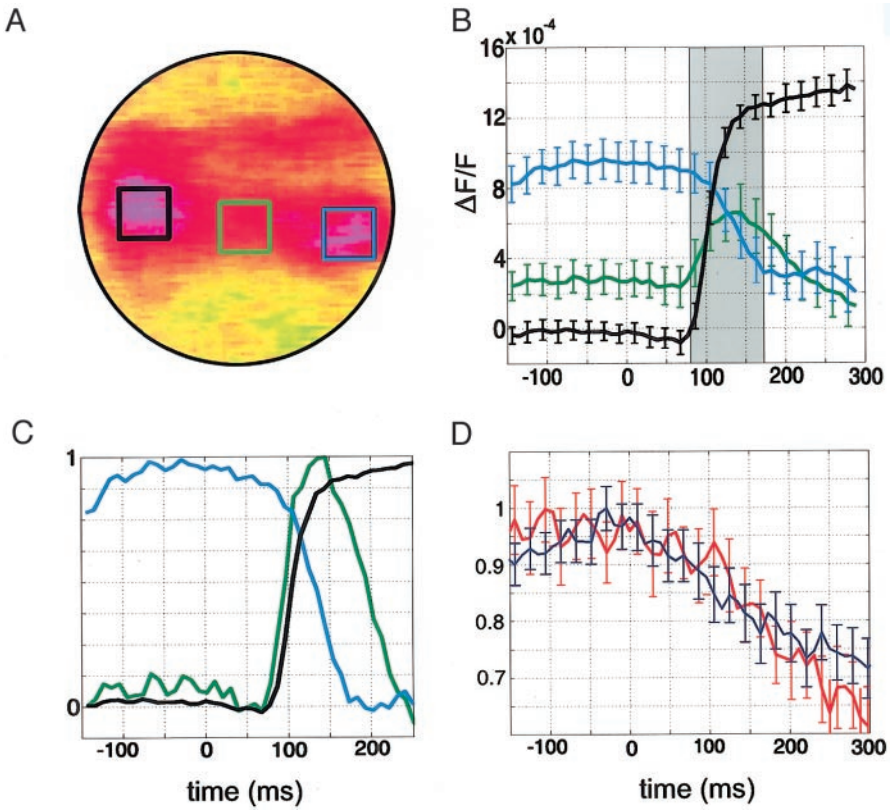

FIG. 11. Response dynamics resulting from a saccadic eye movement and stimulus offset. *A*: 3 different regions in area V1 of *monkey M* are marked on a map showing the activation before and after a saccade (marked with different colored squares). Data are the same as in Fig. 10*B*. *B*: time course of the evoked activity from these 3 different locations after onset of a saccade to the visual stimulus. Errors bars represent 1 SE and are plotted for every 2nd sample point ($n = 17$ trials). The time course in cyan shows the cortical response calculated from the region that responded initially to the onset of the local visual stimulus (cyan square in *A*). After saccadic onset, the response gradually decreased. The region enclosed in the black square, responded only after the saccadic eye movement. The gray area marks the temporal overlap of ~100 ms between the evoked responses in these 2 retinotopically activated regions. Following the saccade, the region enclosed in the green square was activated more weakly by the visual stimulus passing through its retinotopical coordinates, relative to the activation in the region where the stimuli reached its retinotopical coordinates at the end of the saccade (marked in black). *C*: time course of responses shown in *B*, normalized to the maximal response amplitude. Activation of the green response starts before the response in black. *D*: average cortical response fall-off after a saccade to a visual stimulus (blue, $t = 0$ is the onset of saccade; $n = 20$ trials) and after stimulus offset (red, $t = 0$ is the offset of the visual stimulus; $n = 8$ trials). Data were normalized to the maximal response amplitude; error bars represent 1 SE. For both conditions, the visual stimulus was presented 300−800 ms before saccadic onset or visual stimulus offset.

pattern of functional architecture obtained by intrinsic imaging was preserved. Other observations supported this result: time-course amplitude was preserved across several months of VSDI, behavioral performance of contrast discrimination was not affected by the long-term VSDI, and single-unit recording showed no rough abnormal activity. We therefore conclude that long-term VSDI in behaving monkeys, as implemented here, does not produce significant cortical damage.

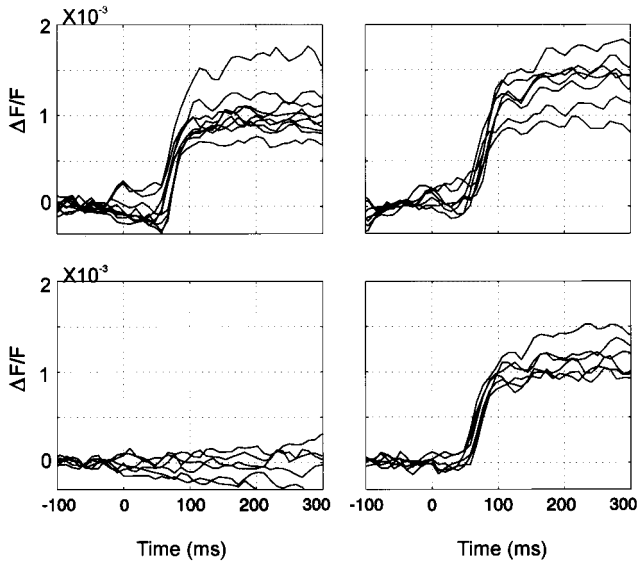

FIG. 12. Evoked response can be detected in single trials. Evoked responses from single trials (*top* and *right bottom*) and blank single trials as a control for the noise level (*left bottom*). All traces were spatially averaged over a small area in V1. All traces were divided by the average blank value. The stimulus was an isoluminant, square drifting grating (size, 0.5 × 0.5°; spatial frequency, 3 cycle/°; temporal frequency, 1°/s; orientation, 0°; located 3.5° below the horizontal meridian and 1.5° from the vertical meridian, stimulus onset at $t = 0$). In the blank condition the monkey was fixating but was not presented with the visual stimulus. Data were weakly low-pass filtered.

Evoked response dynamics

The evoked response latency in area V1 varied between 46 and 68 ms among the different monkeys. These results are in line with previous studies of single- and multiunit recordings that were done in behaving monkeys and showed similar latencies in V1 (Celebrini et al. 1993; Knierim and Van Essen 1992; Maunsell and Gibson 1992; Petersen et al. 1988; Schmolesky et al. 1998; Schroeder et al. 1998; Vogels and Orban 1991).

Another finding of this study was that the decay in the neuronal population response to baseline level after stimulus offset was slower than the increase in neuronal activity from baseline after stimulus onset. This may suggest that the response of the neuronal population is better synchronized during the onset of thalamic input than during the offset, when cortical circuits remain reverberating for a while until the neuronal activity decays and returns to baseline (A. Sterkin, D. Ferster, I. Lampl, A. Arieli, unpublished observations).

A recent work (Bair et al. 2002) has also found that the timing response of onset and offset in monkey's visual neurons is different in latency and stimulus dependence. They also indicated that the onset latency *could be* more variable compared with offset response. However, this was found only for a small population of simple cells ($n = 16$) and could be related to the unique stimulus configuration that was used in this work.

Dynamics of functional domains

Both ocular-dominance and orientation domains developed as soon as the evoked response started (temporal resolution of 9.6 ms/frame). This is in agreement with studies showing that orientation tuning in the macaque primary visual area develops within a short time after stimulus onset (Celebrini et al. 1993; Ringach et al. 1997, Sharon and Grinvald 2002). The similar latencies of ocular-dominance and VH map development suggest not only ocular-dominance selectivity but also orientation selectivity in the organization of thalamic input. The similar dynamics of the ocular-dominance and VH maps (as seen with a temporal resolution of 9.6 ms/frame and the current signal-to-noise ratio) suggest that the ocular-dominance and orientation inputs have similar cortical processing. The present results do not however rule out dynamics in the orientation tuning that is represented in the cortex at early time because of the limited temporal resolution and signal-to-noise ratio of the present orientation maps. Such early changes, revealed by VSDI, were recently reported in the anesthetized cat, where the signal-to-noise ratio was higher (Sharon and Grinvald 2002).

The mapping signal (the differential responses for both orientation and OD) reached its maximal value within 40–50 ms from response onset, whereas the evoked response increased throughout the response and continued to increase until ~250 ms after stimulus onset. Further analysis showed that VSD response latencies were similar between the preferred and nonpreferred orientation as well as between the dominant and nondominant eye. Given the current time resolution of 9.6 ms/frame, we do not rule out that a latency difference smaller than ~10 ms may exist; some difference is expected from the anatomy, at least for the OD case. Indeed, several studies showed some indications for a latency difference between the preferred versus nonpreferred (e.g., Celebrini et al. 1993; Volgushev et al. 1995).

Even at this time resolution we found that the response to the dominant eye or preferred orientation increased faster and reached a larger amplitude relative to that of the nondominant or nonpreferred response, respectively (per definition, it is this difference that produced the mapping signal). Similar results have been reported in Gillespie et al. (2001) and in the recent work of Sharon and Grinvald (2002) (time resolution was 9.6 ms/frame.) It is important to repeat these experiments with higher time resolution.

Intracellular recording have shown that neurons with orientation selectivity responded with an increase of their membrane potential and spiking activity to the preferred orientation. Similarly, the same neurons exhibited subthreshold depolarization to nonpreferred orientation (Gillespie et al. 2001; Volgushev et al. 1995). Thus in a similar way to the orientation, single neurons in layer 2–3 should show depolarization in response to the nondominant eye visual stimulus.

VSDI and imaging based on intrinsic signals: sensitivity to subthreshold and spiking activities

As we showed in the present work, there is clear similarity between the ocular-dominance or VH functional domains obtained by VSDI and those obtained by intrinsic imaging whenever the maps are obtained by differential imaging. Per definition, with differential imaging, the common mode of the responses to orthogonal stimuli is eliminated. The ratio of the evoked signal to the mapping signal is an indication to the relative size of the common mode response. In the case of ocular dominance and orientation, it is well known that the two orthogonal domains both exhibit subthreshold activated in response to the null stimulus. In contrast, suprathreshold activation occurs almost exclusively in response to the optimal stimulus. We found that the fractional change of the mapping signal (for either VH or ocular dominance) is significantly higher for the intrinsic maps than for maps obtained by VSDI (Grinvald et al. 2000; Shtoyerman et al. 2000). This finding indicates that the intrinsic signal obtained at 605 nm is emphasizing suprathreshold activity more than the dye signal and vice versa; the dye signal places more emphasis on subthreshold activity. This possibility is further supported by the observation that the evoked responses of both ocular-dominance and VH stimuli reached their maximal amplitudes only ~100 ms after maximal amplitudes had been reached by the mapping signals, suggestive of reverberating subthreshold synaptic activation.

Response to small localized visual stimuli

VSDI emphasizes subthreshold activity of neuronal populations. It is therefore not surprising that the spatial extent of the evoked cortical response to a small stimulus imaged by VSD (Fig. 9) substantially exceeded that expected by classical techniques, which typically are biased to the suprathreshold activity (Dow et al. 1981; Tootell et al. 1988; Van Essen et al. 1984). The results of the present study are in line with previous findings on the point spread function studied by VSDI in anesthetized monkeys (Grinvald et al. 1994). More recent studies of intracellular recordings showed that the size of the subthreshold receptive field is indeed much larger than the classical or spiking receptive field (Bringuier et al. 1999). Moreover, we showed that the response reached its maximal extent within 30−40 ms, which means that the magnification factor we measured for population synaptic activity was dynamic and increased to its full extent within 30−40 ms after response onset (Fig. 9). The evoked responses to small visual stimuli in V1 were anisotropic close to the vertical meridian, and were similar to those described previously (Dow et al. 1985; Tootell et al. 1988; Van Essen et al. 1984).

Cortical activity after a saccadic eye movement

The rapid optical signal triggered by a saccadic eye movement (Figs. 10 and 11) showed that there is an overlap period of ~100 ms during which the visual cortex simultaneously has two locations of activation but only one visual target appears on the screen. This results from the slow fall-off of the cortical response following cessation of the stimulus. Moreover, we found cortical responses to a small stimulus moving with saccadic velocity as shown by the fact that cortical regions located in the saccadic trajectory responded with a direct transient activation after the saccadic eye movement to the visual target (Fig. 11, *A*, green box, and *B*). It remains to be explored what is the relationship between these transient activations and perception.

In summary, this work lays the foundation for a new way

of recording and analyzing the dynamics of population activity in behaving monkeys, with both a high spatial and temporal resolution. The combination of VSDI with traditional electrical recordings can also be readily adapted for the behaving monkey and would facilitate the selective visualization of neuronal assemblies (Arieli et al. 1995, Tsodyks et al. 1999) involved in dynamic representations and processing of sensory input, as well as in the planning, control, and execution of motor output.

We thank D. Sharon and F. Shavan for reading an earlier version of this manuscript and S. Smith for editing the manuscript.

This work was supported by grants from the Grodetsky Center, the Goldsmith and Glasberg Foundations, and the Korber Foundation.

REFERENCES

ARIELI A, SHOHAM D, HILDESHEIM R, AND GRINVALD A. Coherent spatiotemporal patterns of ongoing activity revealed by real-time optical imaging coupled with single-unit recording in the cat visual cortex. *J Neurophysiol* 73: 2072–2093, 1995.

ARIELI A AND GRINVALD A. Optical imaging combined with targeted electrical recordings, microstimulation, or tracer injections. *J Neurosci Methods* 116: 15–28, 2002.

ARIELI A, GRINVALD A, AND SLOVIN H. Dural substitute for long-term imaging of cortical activity in behaving monkeys and its clinical implications. *J Neurosci Methods* 114: 119–133, 2002.

BAIR W, CAVANAUGH JR, SMITH MA, AND MOVSHON JA. The timing of response onset and offset in macaque visual neurons. *J Neurosci* 22: 3189–3205, 2002.

BATTAGLINI PP, GALLETTI C, AICARDI G, SQUATRITO S, AND MAIOLI MG. Effect of fast moving stimuli and saccadic eye movements on cell activity in visual areas V1 and V2 of behaving monkeys. *Arch Ital Biol* 124: 111–119, 1986.

BONHOEFFER T AND GRINVALD A. The layout of iso-orientation domains in area 18 of cat visual cortex: optical imaging reveals a pinwheel-like organization. *J Neurosci* 13: 4157–4180, 1993.

BORN RT AND TOOTELL RB. Single-unit and 2-deoxyglucose studies of side inhibition in macaque striate cortex. *Proc Natl Acad Sci USA* 88: 7071–7075, 1991.

BRIDGEMAN B, HENDRY D, AND STARK L. Failure to detect displacement of the visual world during saccadic eye movements. *Vision Res* 15: 719–722, 1975.

BRINGUIER V, CHAVANE F, GLAESER L, AND FREGNAC Y. Horizontal propagation of visual activity in the synaptic integration field of area17 neurons. *Science* 283: 695–699, 1999.

CELEBRINI S, THORPE S, TROTTER Y, AND IMBERT M. Dynamics of orientation coding in area V1 of the awake primate. *Vis Neurosci* 10: 811–825, 1993.

CHAKRABORTY S, TUMOSA N, AND LEHMKUHLE S. Visually evoked cortical potentials in awake cats during saccadic eye movements. *Exp Brain Res* 122: 203–213, 1998.

DOW BM, SNYDER AZ, VAUTIN RG, AND BAUER R. Magnification factor and receptive field size in the foveal striate of monkey. *Exp Brain Res* 44: 213–288, 1981.

DOW BM, VAUTIN RG, AND BAUER R. The mapping of visual space onto foveal striate cortex in the macaque monkey. *J Neurosci* 5: 890–902, 1985.

FISCHER B, BOCH R, AND BACH M. Stimulus versus eye-movements: comparison of neural activity in the striate and prelunate visual cortex (A17 and A19) of trained rhesus monkeys. *Exp Brain Res* 43: 69–77, 1981.

GILLESPIE DC, LAMPL I, ANDERSON JS, AND FERSTER D. Dynamics of the orientation-tuned membrane potential response in cat primary visual cortex. *Nat Neurosci* 4: 1014–1019, 2001.

GRINVALD A, ANGLISTER L, FREEMAN, JA, HILDESHEIM R, AND MANKER A. Real-time optical imaging of naturally evoked activity in intact frog brain. *Nature* 308: 848–850, 1984.

GRINVALD A, LIEKE EE, FROSTIG RD, AND HILDESHEIM R. Cortical point-spread function and long-range lateral connections revealed by real-time optical imaging of macaque monkey primary visual cortex. *J Neurosci* 14: 2545–2568, 1994.

GRINVALD A, SHOHAM D, SHMUEL A, GLASER DE, VANZETTA I, SHTOYERMAN E, SLOVIN H, WIJNBERGEN C, HILDESHEIM R, STERKIN A, AND ARIELI A. In vivo optical imaging of cortical architecture and dynamics. In: *Modern Techniques in Neuroscience Research,* edited by Windhorst U and Johansson H. New York: Springer, 1999, p. 893–969.

GRINVALD A, SLOVIN H, AND VANZETTA I. Non-invasive visualization of cortical columns by fMRI. *Nat Neurosci* 3: 105–107, 2000.

HUBEL DH AND WIESEL TN. Receptive fields, binocular interaction and functional architecture in the cat's visual cortex. *J Physiol (Lond)* 160: 106–154, 1962.

HUBEL DH AND WIESEL TN. Anatomical demonstration of columns in the monkey striate cortex. *Nature* 221: 747:750, 1969.

HUBEL DH AND WIESEL TN. Laminar and columnar distrubution of geniculo-cortical fibers in the macaque monkey. *J Comp Neurol* 158: 267–294, 1972.

KNIERIM JJ AND VAN ESSEN DC. Neuronal responses to static texture patterns in area V1 of the alert macaque monkey. *J Neurophysiol* 67: 961–980, 1992.

LATOUR PL. Visual threshold during eye movements. *Vis Res* 2: 261–262, 1962.

MAUNSELL JH AND GIBSON JR. Visual response latencies in striate cortex of the macaque monkey. *J Neurophysiol* 68: 1332–1344, 1992.

MACKAY DM. Elevation of visual threshold by displacement of visual images. *Nature* 225: 90–92, 1970.

MOUNTCASTLE VB. Modality and topographic properties of single neurons of cat's somatosensory cortex. *J Neurophysiol* 20: 408–434, 1957.

PETERSEN CC AND SAKMANN B. Functionally independent columns of rat somatosensory barrel cortex revealed with voltage-sensitive dye imaging. *J Neurosci* 21: 8435–8446, 2001.

PETERSEN SE, MIEZIN FM, AND ALLMAN JM. Transient and sustained responses in four extrastriate visual areas of the owl monkey. *Exp Brain Res* 70: 55–60, 1988.

RIGG LA. Suppression of visual phosphenes during saccadic eye-movements. *Vis Res* 14: 997–1011, 1974.

RINGACH DL, HAWKEN M, AND SHAPLEY R. Dynamics of orientation tuning in macaque primary visual cortex. *Nature* 387: 281–284, 1997.

ROSS J, MORRONE MC, GOLDBERG ME, AND BURR DC. Changes in visual perception at the time of saccades. *Trends Neurosci* 24: 113–121, 2001.

SALZBERG BM, DAVILA HV, AND COHEN LB. Optical recording of impulses in individual neurons of an invertebrate central nervous system. *Nature* 246: 508–509, 1973.

SCHMOLESKY MT, WANG Y, HANES DP, THOMPSON KG, LEUTGEB S, SCHALL JD, AND LEVENTHAL AG. Signal timing across the macaque visual system. *J Neurophysiol* 79: 3272–3278, 1998.

SCHROEDER CE, METHA AD, AND GIVRE SJ. A spatiotemporal profile of visual system activation revealed by current source density analysis in the awake monkey. *Cereb Cortex* 8: 575–592, 1998.

SEIDEMANN E, ARIELI A, GRINVALD A, AND SLOVIN H. Dynamics of depolarization and hyperpolarization in the frontal cortex and saccade goal. *Science* 295: 862–865, 2002.

SHARON D AND GRINVALD A. Dynamics and constancy in cortical spatiotemporal patterns of orientation processing. *Science* 295: 512–515, 2002.

SHOHAM D, GLASER DE, ARIELI A, KENET T, WIJNBERGEN C, TOLEDO Y, HILDESHEIM R, AND GRINVALD A. Imaging cortical dynamics at high spatial and temporal resolution with novel blue voltage-sensitive dyes. *Neuron* 24: 791–802, 1999.

SHTOYERMAN E, ARIELI A, SLOVIN H, VANZETTA I, AND GRINVALD A. Long-term optical imaging and spectroscopy reveal mechanisms underlying the intrinsic signal and stability of cortical maps in V1 of behaving monkeys. *J Neurosci* 20: 8111–8121, 2000.

SLOVIN H, ARIELI A, AND GRINVALD A. Voltage-sensitive dye imaging reveals that behavioral context affects population activity in early visual cortex. *Soc Neurosci Abstr* 26: 1082, 2000a.

SLOVIN H, ARIELI A, HILDESHEIM R, AND GRINVALD A. Long-term voltage-sensitive dye imaging in the behaving monkey. *Soc Neurosci Abstr* 25: 784, 1999.

SLOVIN H, ARIELI A, HILDESHEIM R, AND GRINVALD A. Long-term voltage-sensitive dye imaging in area V1 and V2 of the behaving monkey. *Eur J Neurosci* 12: 126, 2000b.

STERKIN A, LAMPL I, FERSTER D, GLASER DE, GRINVALD A, AND ARIELI A. Interaction between on-going and evoked membrane potential of a single neuron results in a decrease of correlation with the population activity recorded optically. *5th IBRO World Congress of Neuroscience Abstr,* 122, 1999.

STUART GJ AND SAKMANN B. Active propagation of somatic action potentials into neocortical pyramidal cell dendrites. *Nature* 367: 69–72, 1994.

THIELE A, HENNING P, KUBISCHIK M, AND HOFFMANN KP. Neural mechanisms of saccadic suppression. *Science* 295: 2460–2462, 2002.

TOOTELL RB, SWITKES E, SILVERMAN MS, AND HAMILTON SL. Functional anatomy of macaque striate cortex. II. Retinotopic organization. *J Neurosci* 8: 1531–1568, 1988.

TSODYKS M, KENET T, GRINVALD A, AND ARIELI A. Linking spontaneous activity of single cortical neurons and the underlying functional architecture. *Science* 286: 1943–1946, 1999.

VAN ESSEN DC, NEWSOME WT, AND MAUNSELL JH. The visual field representation in striate cortex of the macaque monkey: asymmetries, anisotropies, and individual variability. *Vision Res* 24: 429–448, 1984.

VOGELS R AND ORBAN GA. Quantitative study of striate single unit responses in monkeys performing an orientation discrimination task. *Exp Brain Res* 84: 1–11, 1991.

VOLKMAN FC. Vision during saccadic eye movements. *J Opt Soc Am* 52: 571–578, 1962.

VOLGUSHEV M, VIDYASAGAR TR, AND PEI X. Dynamics of the orientation tuning of postsynaptic potentials in the cat visual cortex. *Vis Neurosci* 12: 621–628, 1995.

WURTZ RH. Visual cortex neurons: response to stimuli during rapid eye movements. *Science* 162: 1148–1150, 1968.

WURTZ RH. Comparison of the effects of eye-movements and stimulus movements on striate cortex neurons of the monkey. *J Neurophysiol* 32: 69–77, 1969a.

WURTZ RH. Response of striate cortex neurons to stimuli during rapid eye movements in the monkey. *J Neurophysiol* 32: 975–986, 1969b.

ZUBER B AND STARK L. Saccadic suppression: elevation of visual threshold associated with saccadic eye-movements. *Exp Neurol* 16: 65–79, 1966.